

CHAPTER V

RESULTS AND DISCUSSION

This chapter is divided into seven sections. Section 5.1 reports the compositions and BET surface area of the catalysts. Section 5.2 describes the results of X-ray diffraction pattern (XRD) and IR spectra from Fourier Transform Infrared (FT-IR) analysis. Surface acidity of the catalysts are shown in section 5.3. Effect of tungsten and potassium added on V_2O_5/TiO_2 catalysts, loading sequence of tungsten and potassium added on V_2O_5/TiO_2 catalysts, role of tungsten and potassium on the catalysts and catalytic behavior of the catalysts are presented in sections 5.4, 5.5, 5.6 and 5.7, respectively.

5.1 Compositions and BET surface areas of the catalysts

The compositions and BET surface areas of the catalysts measured by atomic absorption spectroscopy (AAS) and BET surface area, are shown in table 5.1 below.

The data in table 5.1 shows that when the additives (tungsten and/or potassium) are added on the based catalyst, the catalyst surface area slightly changes. Thus, the additive adding slightly affects the surface area of 25 wt.% V_2O_5 . The exceptions are co-25V10W and 25V5W3K. The surface areas of both catalysts differ from other catalysts. Possibly, too high loading results in decreasing of surface area.

Table 5.1: The compositions and BET surface areas of the catalysts

| Samples | BET surface area (m ² /g) | Metal loading (%) | | |
|------------------------------------|---|-------------------|----------|-----------|
| | | Vanadium | Tungsten | Potassium |
| Pure TiO ₂ | 11.88 | - | - | - |
| 25V | 9.87 | 23 | - | - |
| co-25V2W | 12.31 | 23 | 1.7 | - |
| 5W25V | 12.59 | 21 | 2.4 | - |
| 25V5W | 10.05 | 21 | 3.4 | - |
| co-25V5W | 12.44 | 23 | 3.5 | - |
| co-25V10W | 6.99 | 22 | 6.8 | - |
| co-25V1K | 10.2 | 22 | - | 0.9 |
| 3K25V | 10.91 | 22 | - | 2.4 |
| 25V3K | 9.21 | 21 | - | 2.4 |
| co-25V3K | 10.91 | 22 | - | 2.5 |
| co-25V5K | 10.12 | 21 | - | 4.2 |
| 25V5W3K | 6.87 | 21 | 2.8 | 2.1 |
| pure V ₂ O ₅ | 10.40 | 100 | - | - |

Remarks: the value showed in the symbols of samples are the amounts that loaded on the catalysts. The amounts which exist on the catalysts are less than the value showed in the symbols of samples.

5.2 XRD and FT-IR analysis

The X-ray diffraction patterns of all catalysts are depicted in figures 5.1-5.16. The crystalline V_2O_5 appears for the 25V based catalyst. For the ternary catalysts, crystalline of tungsten oxide and potassium oxide were not observed. This may be because the amount of W and K was too low. Moreover, the calcination temperature on the catalysts which added tungsten was lower than 750°C (1023 K) in moist air, therefore the crystalline of tungsten could not formed on the catalysts. [Engweiler *et al.* (1996)] In addition, the reason for the crystalline of tungsten and potassium was not found on 25V5W3K catalyst liked the previous case.

Results of FT-IR spectra of all catalysts are exhibited in figures 5.17 – 5.32. The major IR bands of the anatase phase of TiO_2 appear at about 640 cm^{-1} (figure 5.17) while the major IR bands of V_2O_5 exhibit around 614, 833 and 1022 cm^{-1} (figure 5.18). When loaded V_2O_5 25 wt.% on the support TiO_2 , the characteristic IR band of TiO_2 gradually disappears and can not be observed. The disappearance of TiO_2 IR bands show that the surface of TiO_2 is highly covered by V_2O_5 surface species. On 25V catalyst two prominent IR bands around 1022 cm^{-1} and 833 cm^{-1} can be observed (figure 5.21) which can be assigned to the V=O stretching vibration of bulk V_2O_5 and characteristic vibration of V_2O_5 , respectively. [Teratrakoonwicha (1996)]

The IR absorption spectra of the ternary catalysts, co-25V2W, 25V5W, 5W25V and co-25V5W, are not different with that of 25V catalyst. In addition, a band around 816 cm^{-1} , characteristic of stretching W=O (figure 5.19) [Ramis *et al.* (1992)], can not be observed in the catalysts. Excluding co-10W25V catalyst, the band around 833 cm^{-1} can not be observed in this catalyst. Possibly, excess tungsten loading can change electronic properties of the catalyst surface. [Witko *et al.* (1997)] As a result, the band around 833 cm^{-1} disappears. At present there is no explanation for this phenomena.

On the other hand, when 1 wt.% K_2O was added to the based catalyst, the IR band of co-25V1K is similar to 25V catalyst while the three type of 25 wt.% V_2O_5 - 3 wt.% K_2O/TiO_2 catalysts show IR spectra with some differences. The bands of 3K25V exhibit around 1022, 1007 and 972 cm^{-1} while the spectrum of 25V3K shows a shoulder peak around 1022 cm^{-1} . The spectrum of co-3K25V exhibits sharp peak around 1022 cm^{-1} , a small peak around 972 cm^{-1} and a shoulder peak around 833 cm^{-1} . The different order of the introduction of potassium induces a different type of vanadium-containing species. In 3K25V catalyst, V_2O_5 and polymeric $[V-O-V]_n$ species are formed, whereas potassium vanadates KV_3O_8 can form as an additional species on 25V3K catalyst. [Courcot *et al.* 1997] Regarding co-25V5K catalyst (figure 5.31), this catalyst displays the different IR band compared with the based catalyst. That means some new species are formed on this catalyst.

The IR band of the last catalyst, 25V5W3K, is not similar to the previous catalysts. It is composed of 4 peaks that exhibit at 1007, 1006, 990 and 941 cm^{-1} (figure 5.32). It is possible that some new species are formed on 25V5W3K catalyst but not like on 25V5K catalyst.

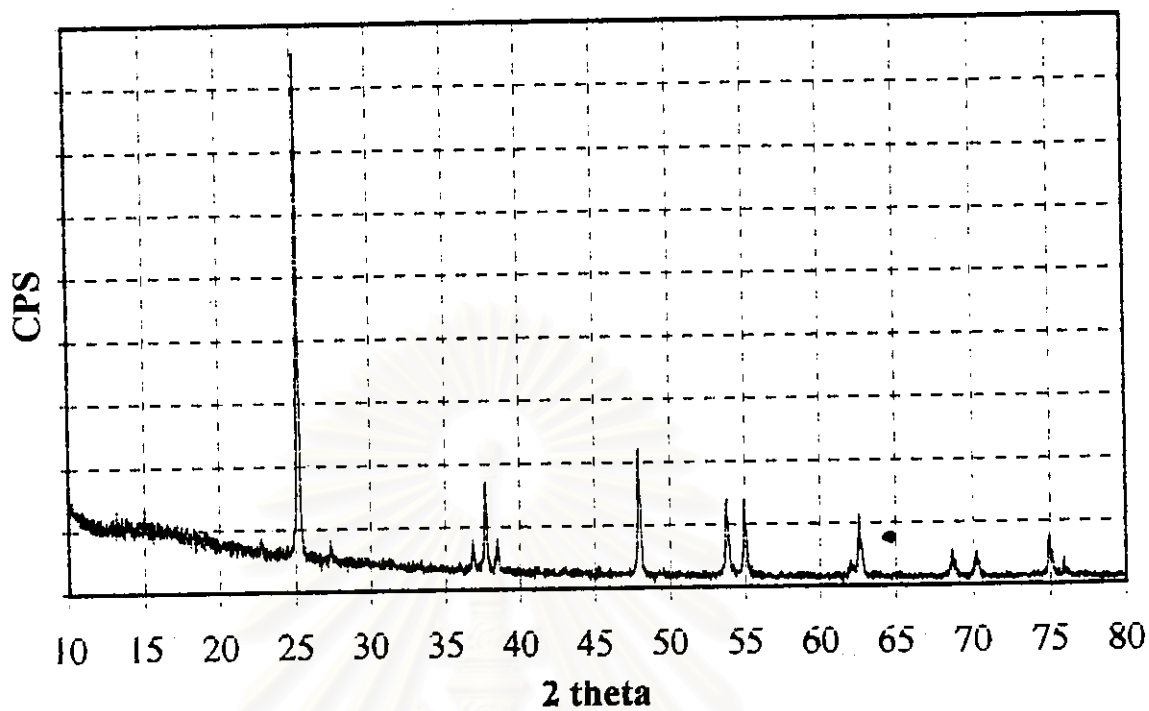


Figure 5.1: XRD pattern of pure TiO_2

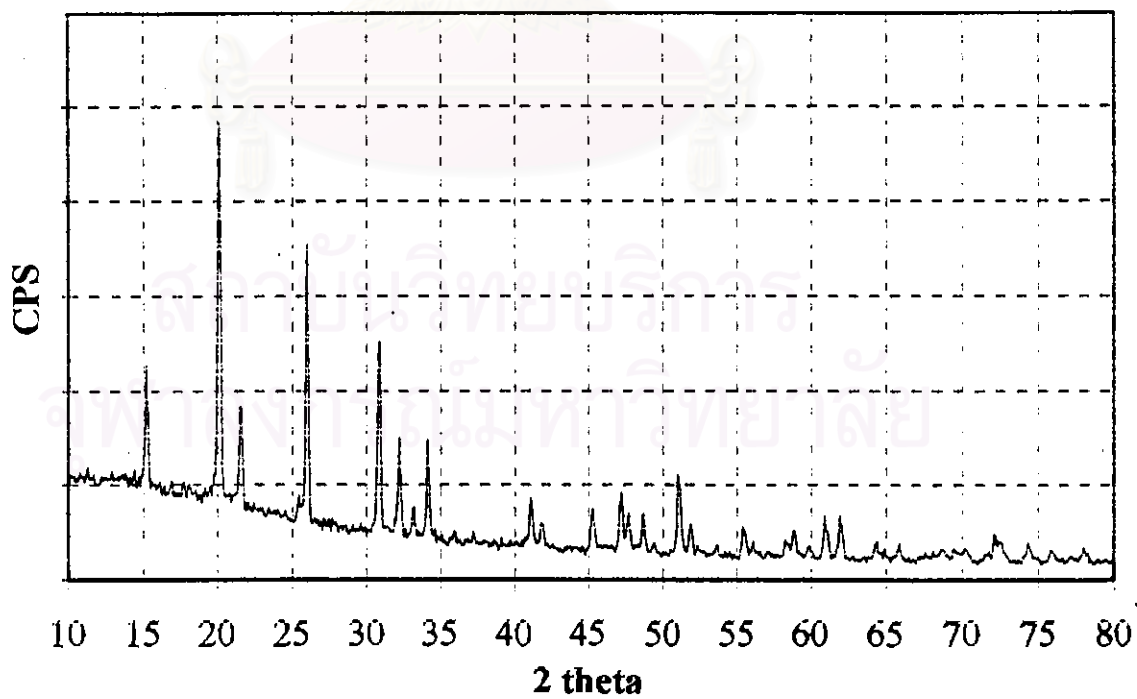


Figure 5.2: XRD pattern of pure V_2O_5

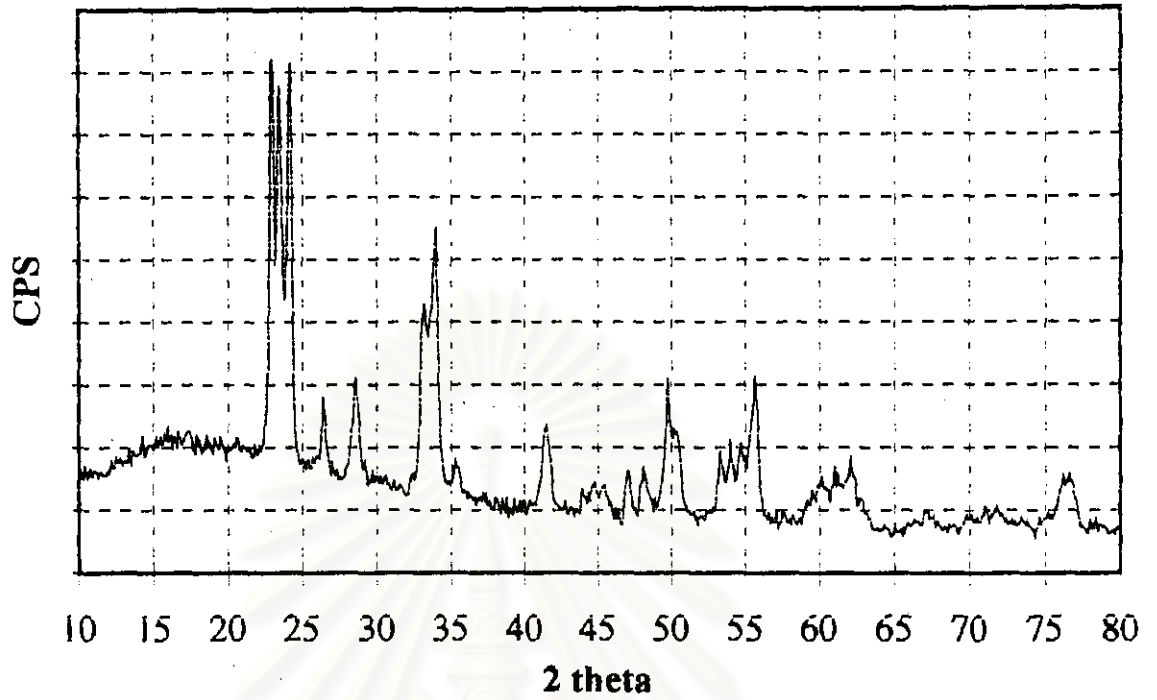


Figure 5.3: XRD pattern of pure WO_3

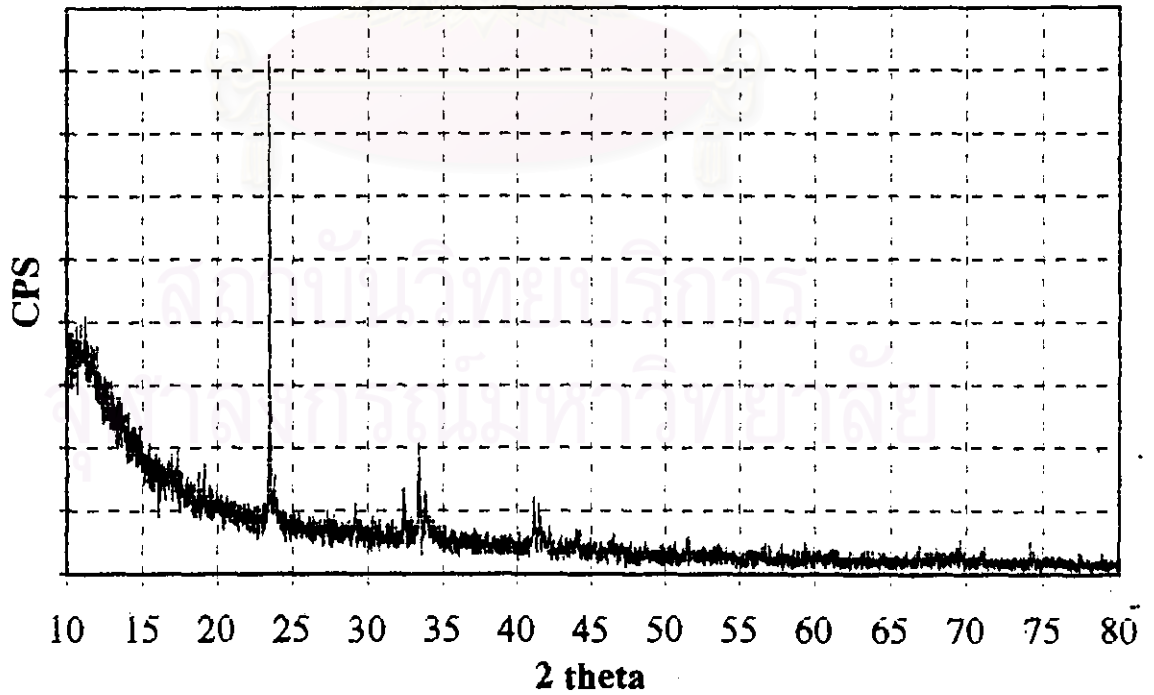


Figure 5.4: XRD pattern of pure K_2O

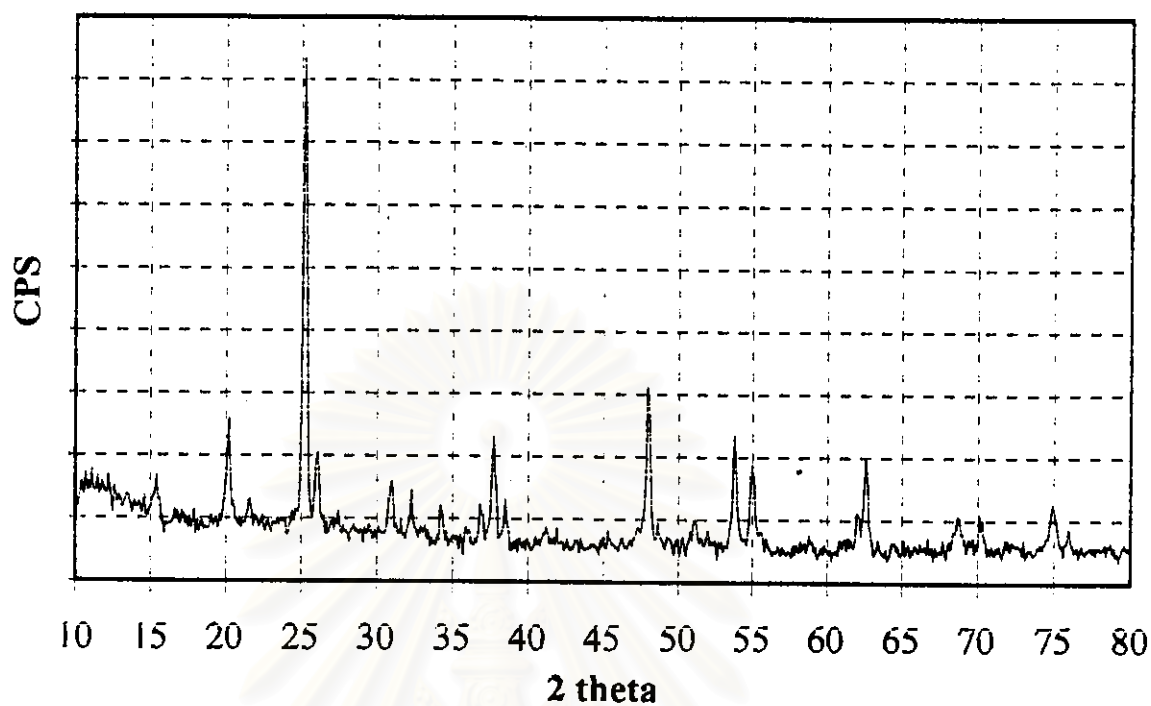


Figure 5.5: XRD pattern of 25V catalyst

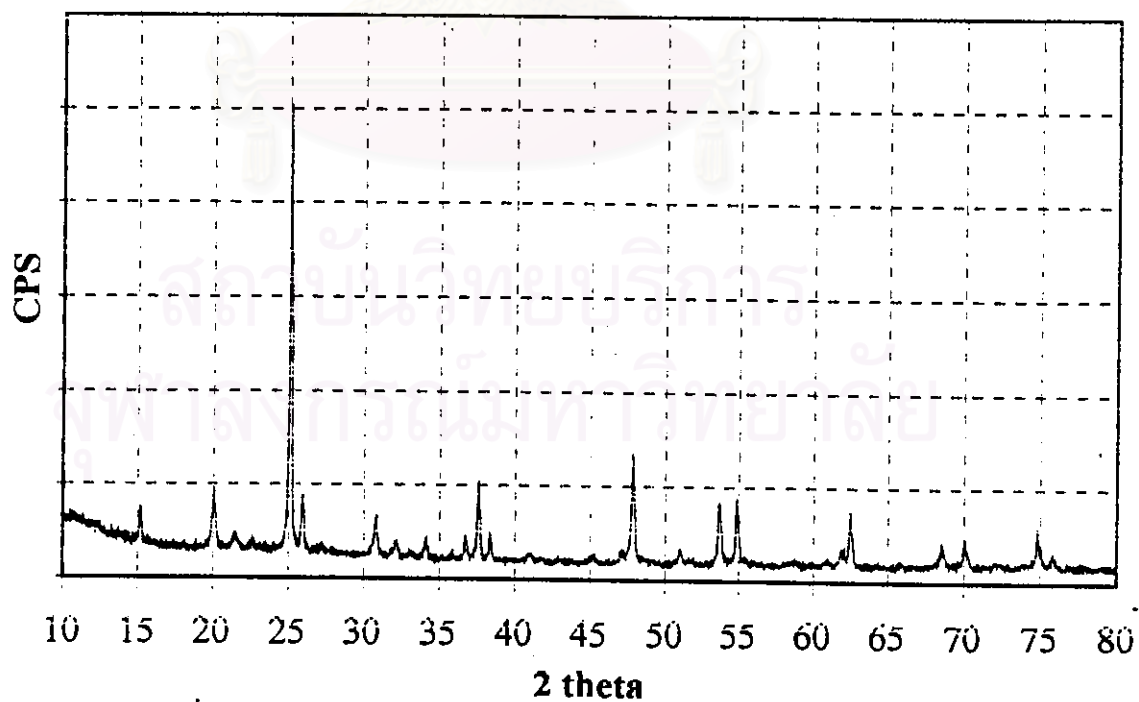


Figure 5.6: XRD pattern of co-25V2W catalyst

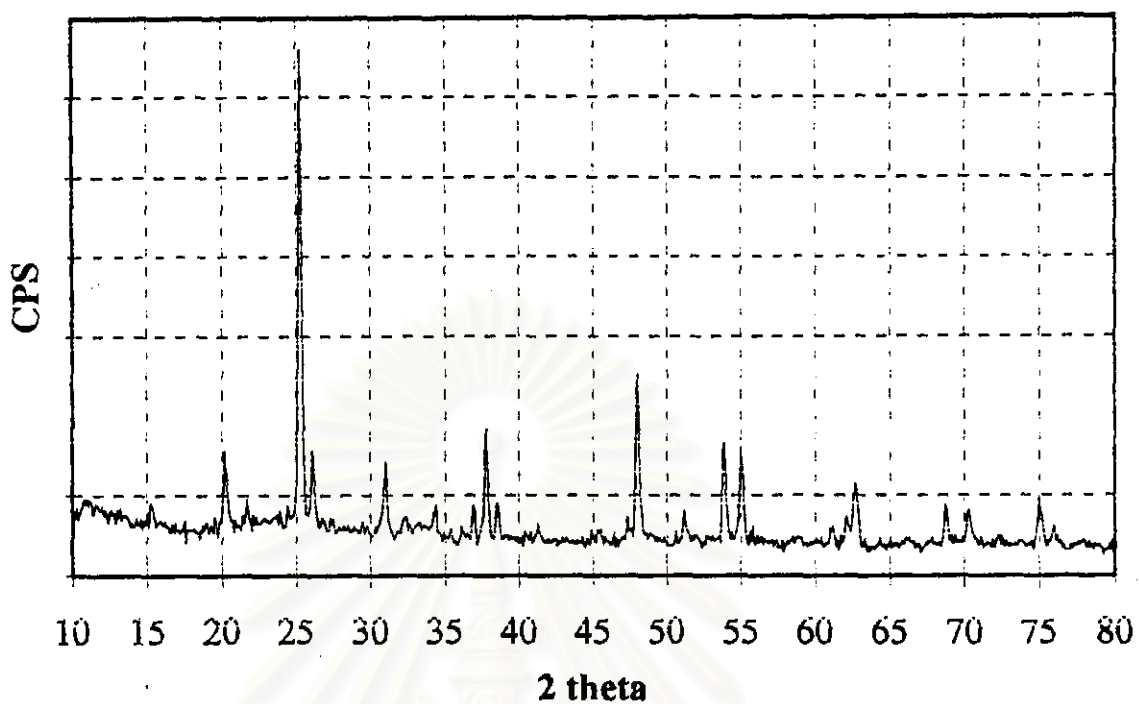


Figure 5.7: XRD pattern of co-25V5W catalyst

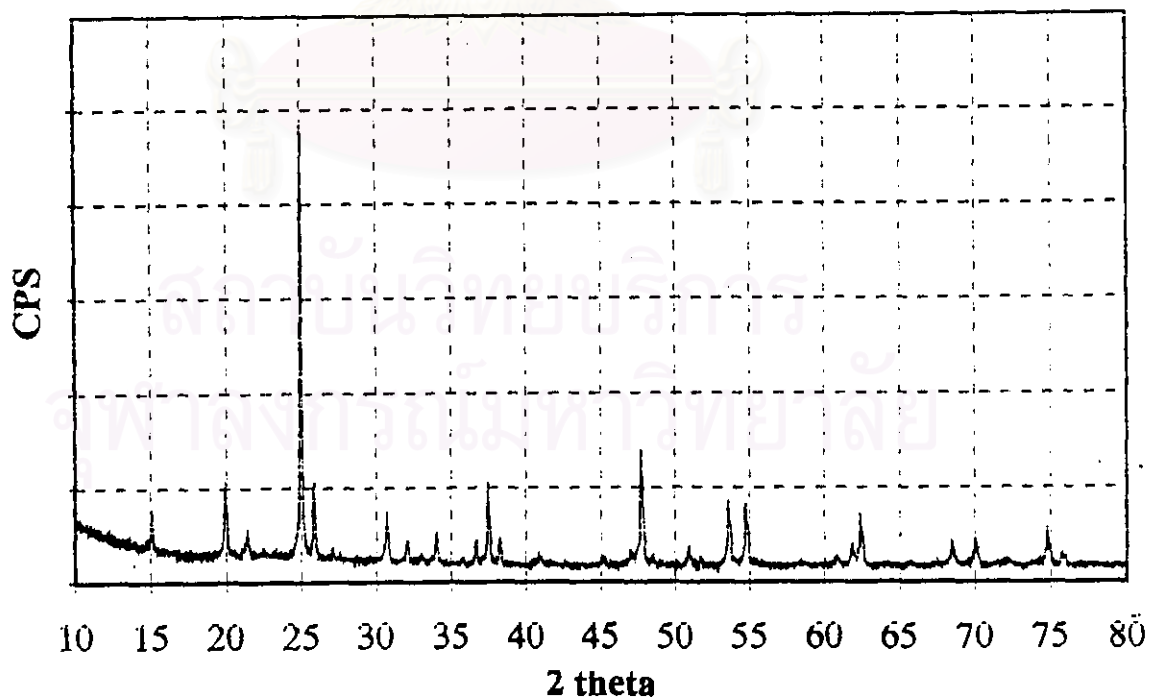


Figure 5.8: XRD pattern of 25V5W catalyst

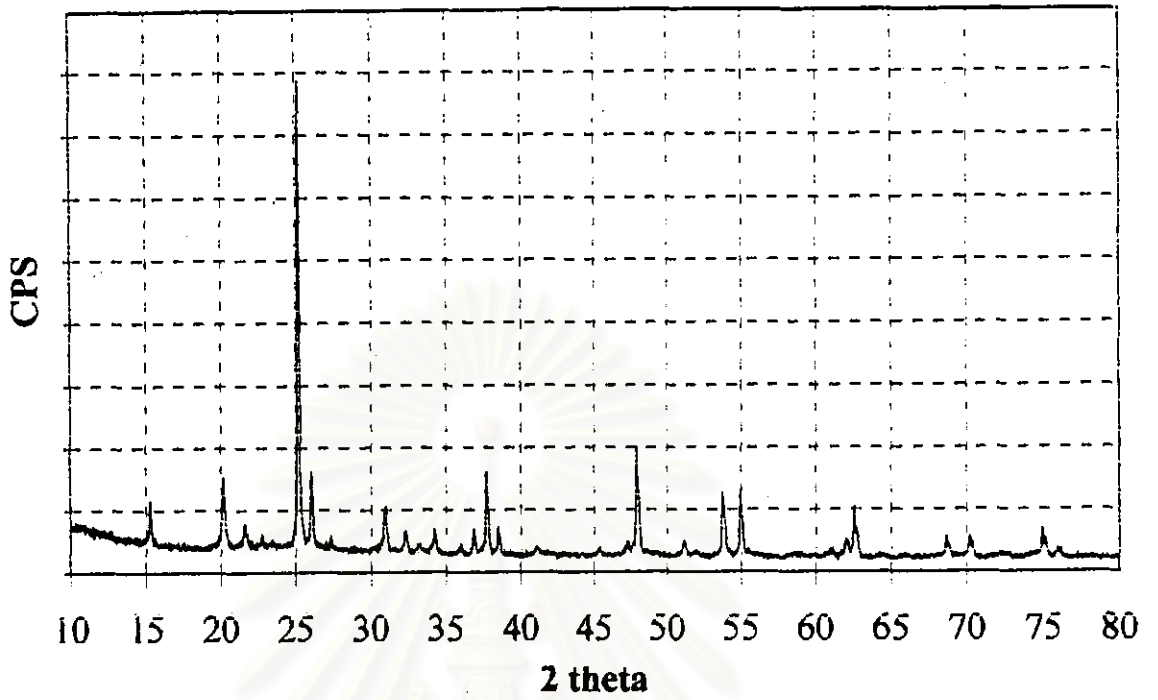


Figure 5.9: XRD pattern of 5W25V catalyst

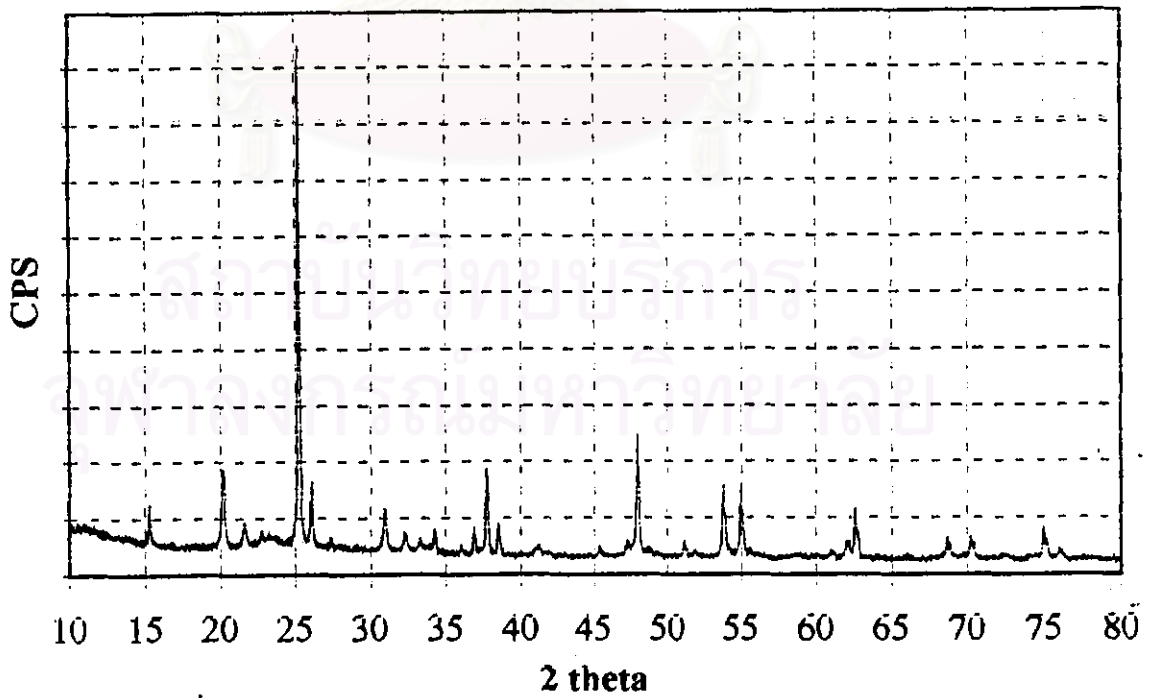


Figure 5.10: XRD pattern of co-10W25V catalyst

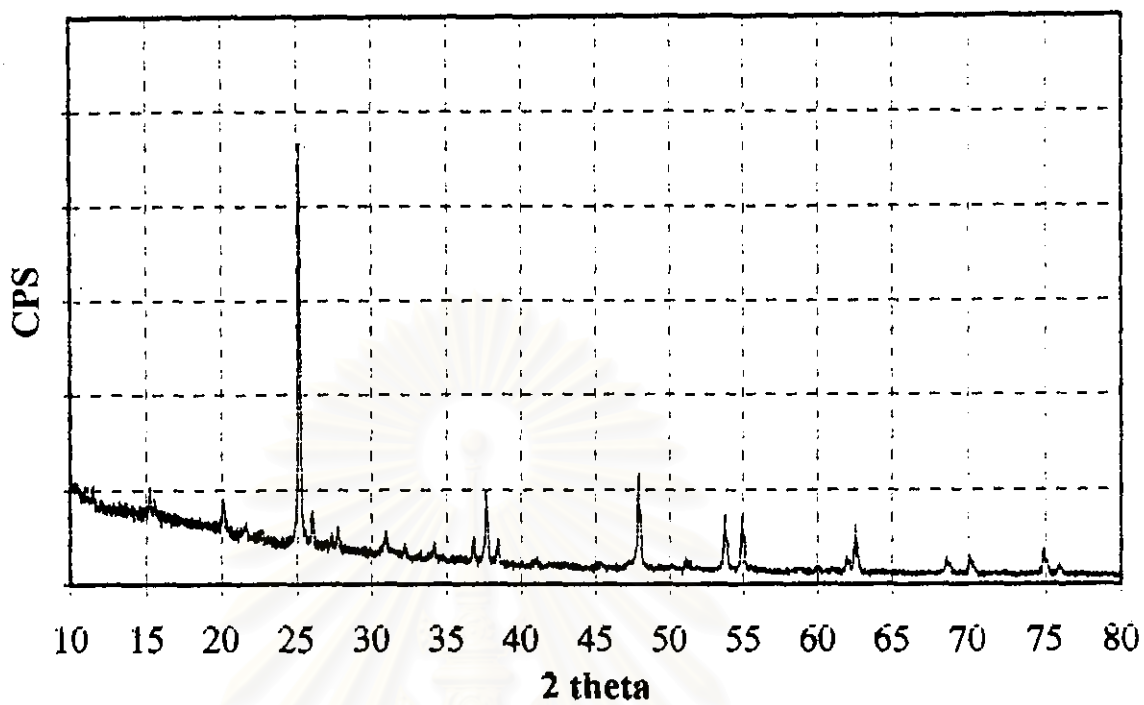


Figure 5.11: XRD pattern of co-25V1K catalyst

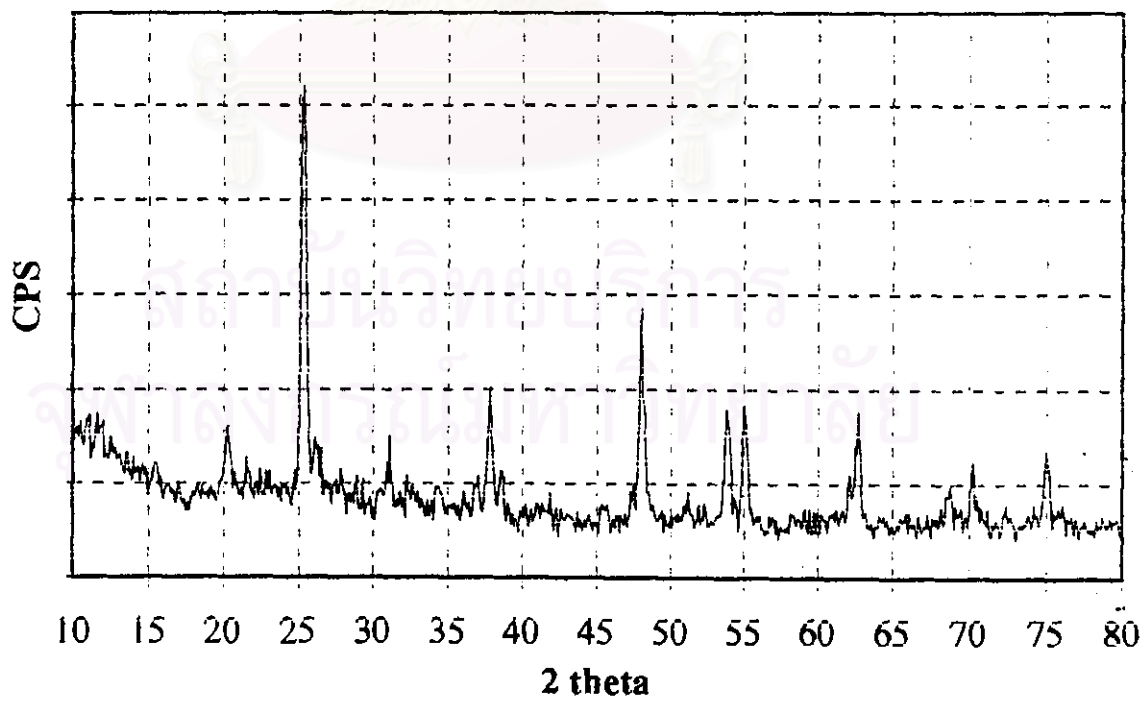


Figure 5.12: XRD pattern of co-25V3K catalyst

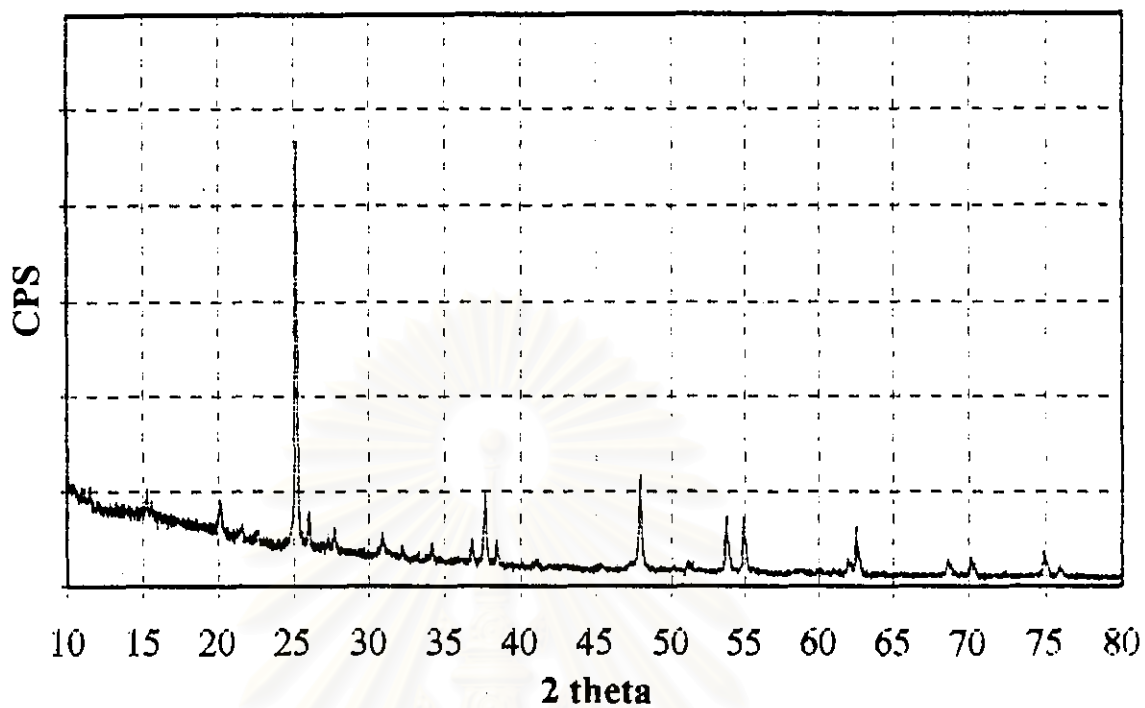


Figure 5.13: XRD pattern of 25V3K catalyst

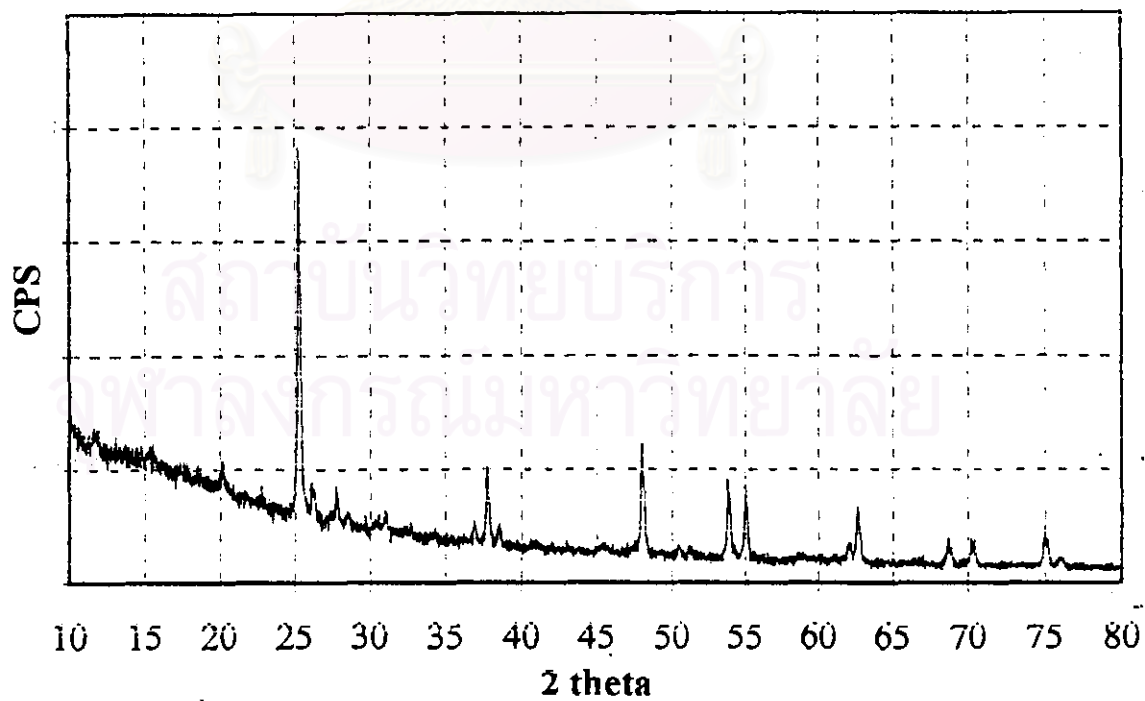


Figure 5.14: XRD pattern of 3K25V catalyst

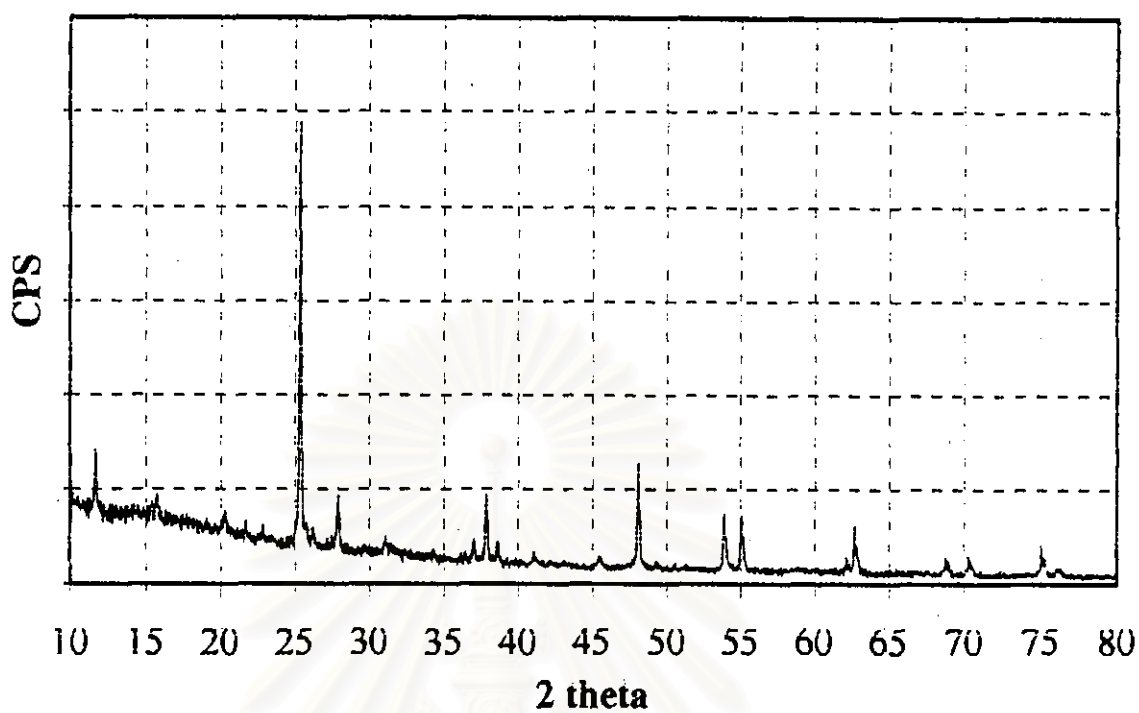


Figure 5.15: XRD pattern of co-25V5K catalyst

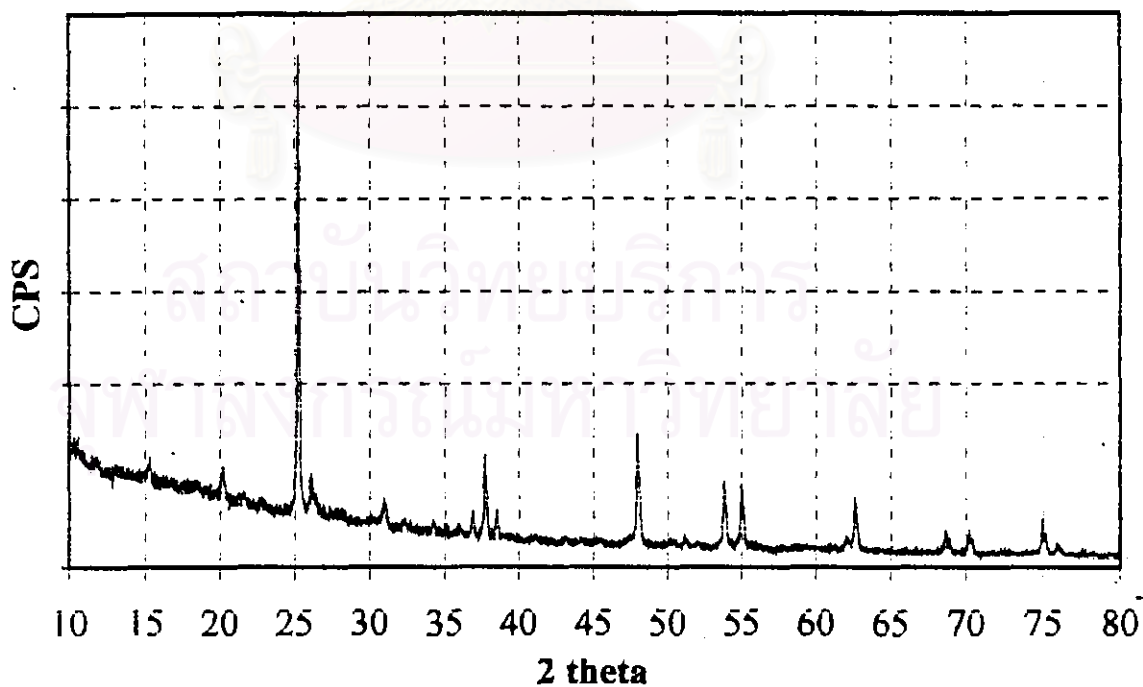


Figure 5.16: XRD pattern of 25V5W3K

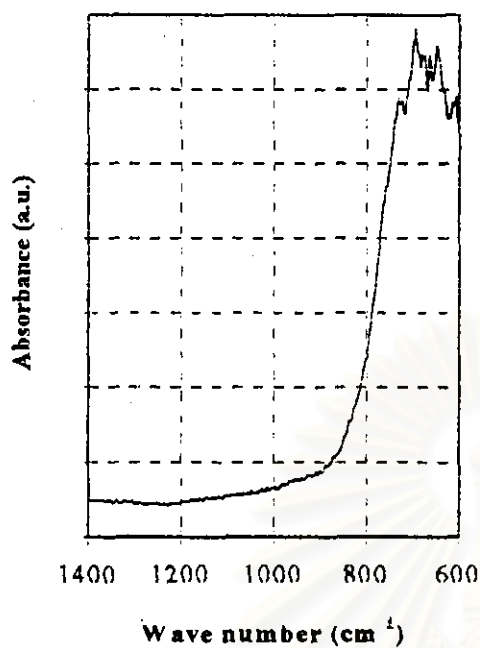


Figure 5.17: IR spectra of pure TiO_2

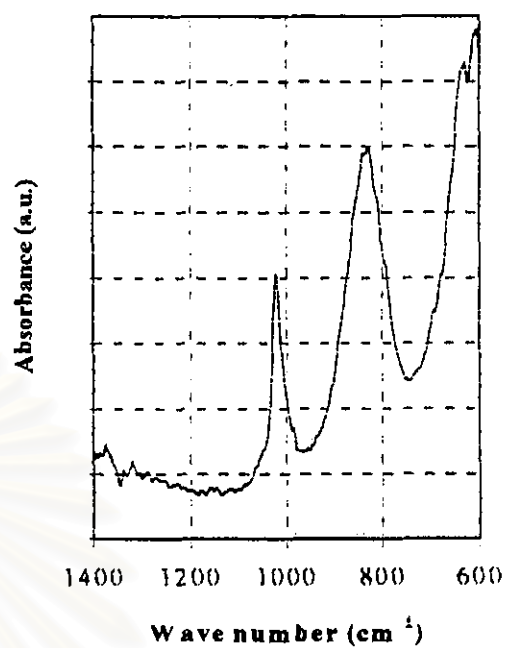


Figure 5.18: IR spectra of pure V_2O_5

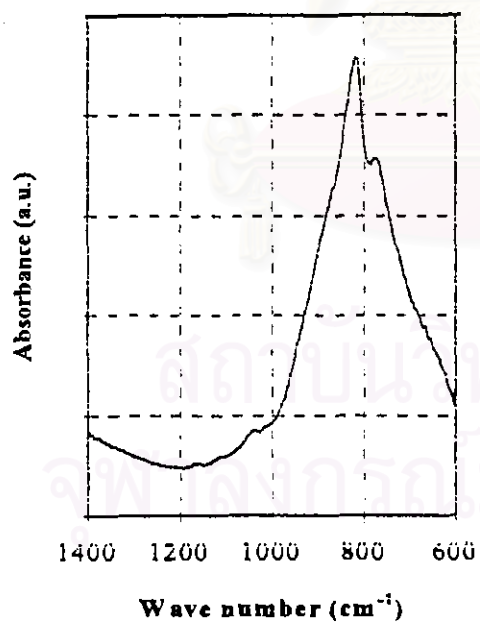


Figure 5.19: IR spectra of pure WO_3

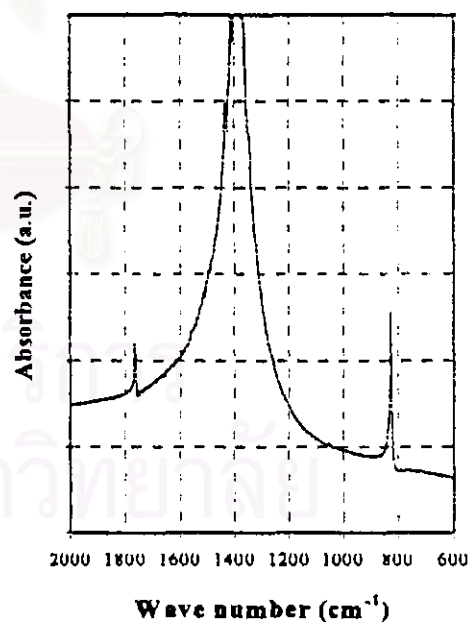


Figure 5.20: IR spectra of pure K_2O

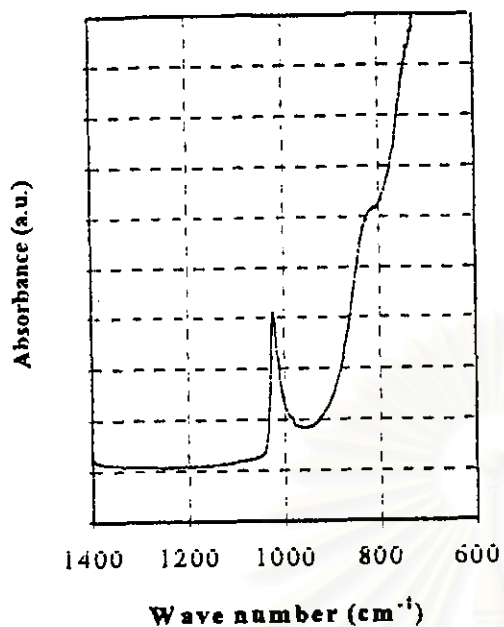


Figure 5.21: IR spectra of 25V catalyst

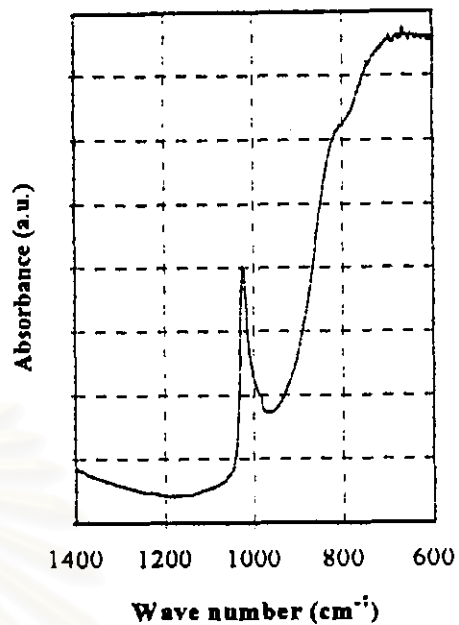


Figure 5.22: IR spectra of co-25V2W catalyst

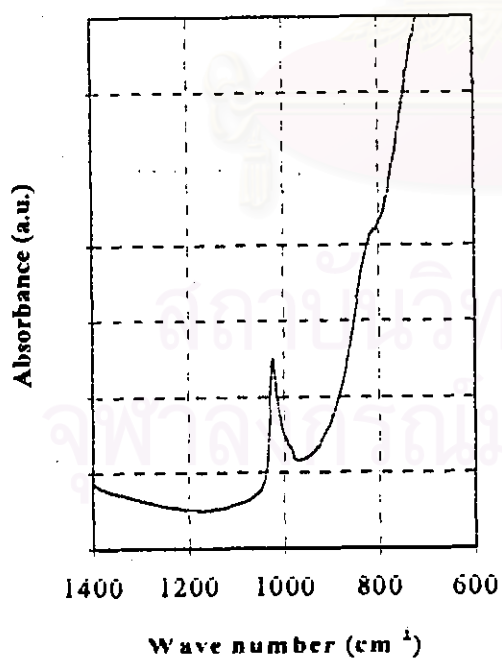


Figure 5.23: IR spectra of co-25V5W catalyst

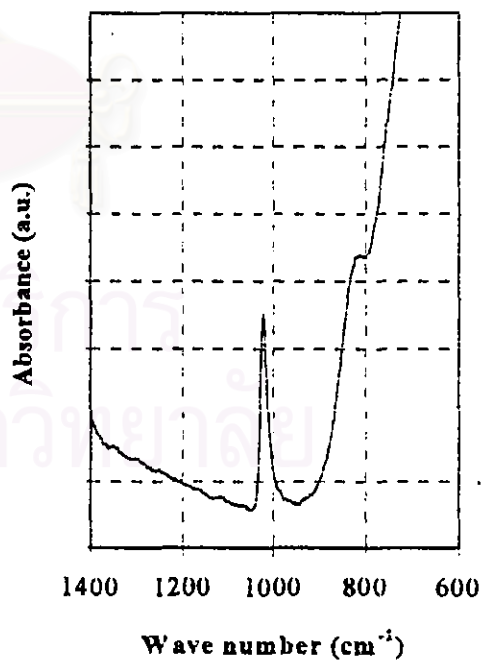


Figure 5.24: IR spectra of 25V5W catalyst

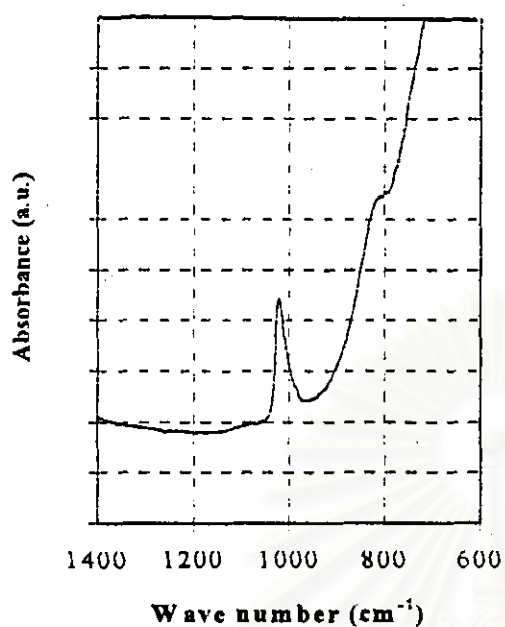


Figure 5.25: IR spectra of 5W25V catalyst

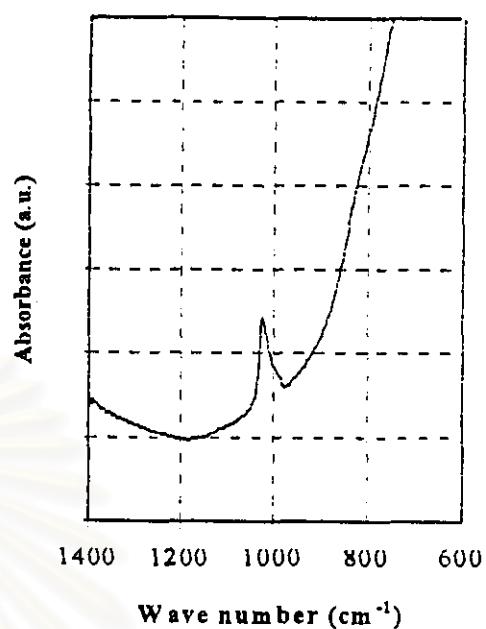


Figure 5.26: IR spectra of co-25V10W catalyst

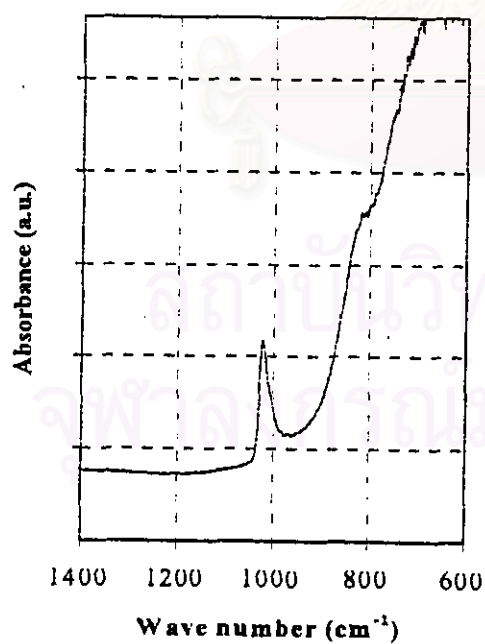


Figure 5.27: IR spectra of co-25V1K catalyst

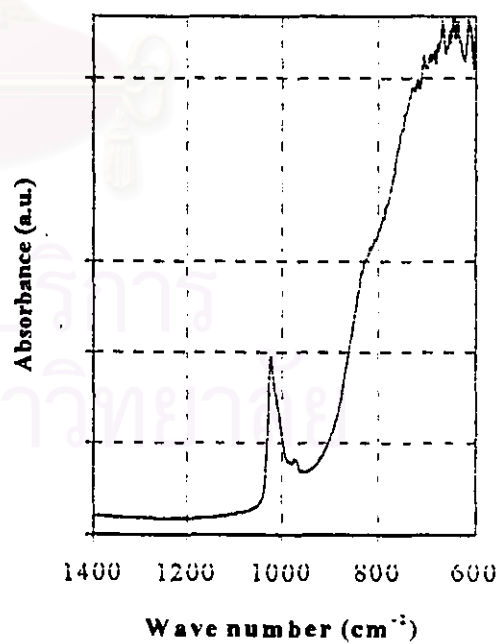


Figure 5.28: IR spectra of co-25V3K catalyst

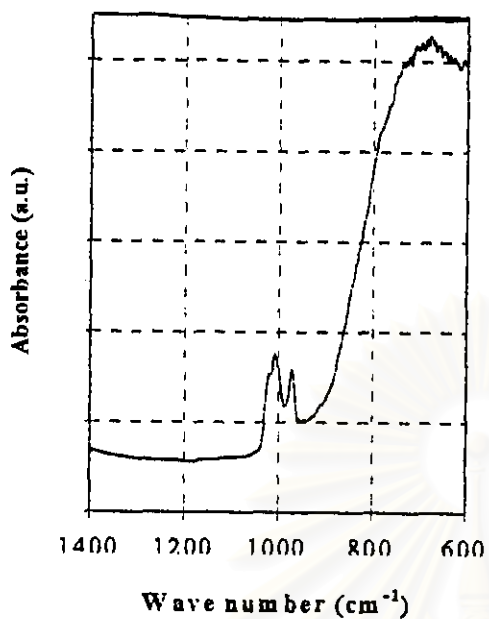


Figure 5.29: IR spectra of 25V3K catalyst

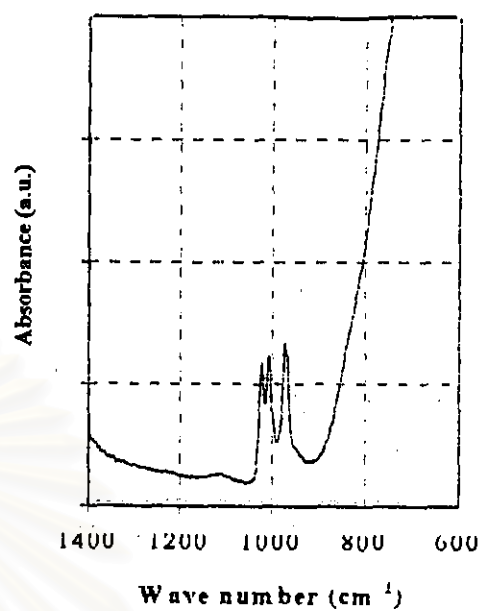


Figure 5.30: IR spectra of 3K25V catalyst

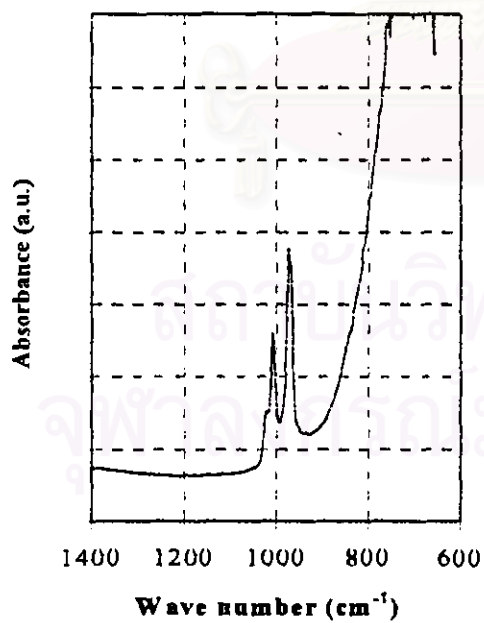


Figure 5.31: IR spectra of co-25V5K catalyst

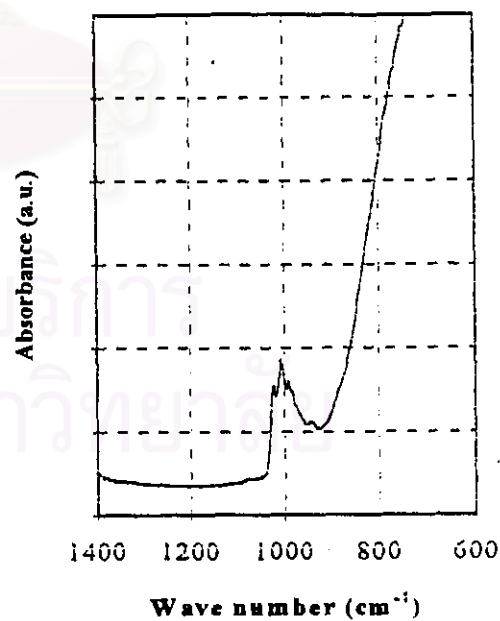


Figure 5.32: IR spectra of 25V5W3K catalyst

5.3 Surface acidity of catalysts

IR spectra of pyridine adsorbed on fresh catalysts are shown in figures 5.33 – 5.41. The band around 1450 cm^{-1} is assigned to molecularly coordinated species, pyridine adsorbed on Lewis acid site. Another important band is the band around 1540 cm^{-1} . This band belongs to protonated species, normally used to indicate the presence of Brønsted acid site. On 25 wt. $\text{V}_2\text{O}_5/\text{TiO}_2$ (figure 5.33), the intensity of the molecularly coordinated species (1450 cm^{-1}) is more than the protonated species (1540 cm^{-1}). After heating under evacuation at room temperature, the peak of the molecularly coordinated species declines faster than the peak of the protonated species but the peak of the protonated species disappears at lower temperature. The pyridinium adsorbed on Brønsted acid sites can not be observed around 250°C , whereas the coordinated pyridine is still detectable and completely disappears around 300°C . This result means that the Lewis acid site is stronger than the Brønsted acid site. This clearly indicates that protonated NH_4^+ species are thermally less stable than molecularly coordinated species. [Lietti *et al.* (1996b), Ramis *et al.* (1996)] In the same way, the spectra of co-25V2W are similar to the spectra of based catalyst (figure 5.34).

Regarding three types of 5 wt.% WO_3 - 25 wt.% $\text{V}_2\text{O}_5/\text{TiO}_2$ catalysts, the peak of the protonated species in co-25V5W is stronger than that of the binary catalyst, including 25V5W, 5W25V catalysts (figures 5.35 - 5.37). After raising up the temperature of 25V, 25V5W, 5W25V catalysts, the peak of the protonated species drops and disappears about 250°C while in co-25V5W it still appears. This result indicates that the acid strength of Brønsted acid site is increased with the presence of W in co-loading method while the band of the coordinatively adsorbed pyridine (1450 cm^{-1}) seems to be relatively constant in three types of 5 wt.% WO_3 - 25 wt.% $\text{V}_2\text{O}_5/\text{TiO}_2$ catalysts. However, 25V, 25V5W, 5W25V and co-25V5W catalysts seem to show small differences in acid strength. In addition, the amount of acid site is a significant factor. Because the amount of Lewis acid site on 25V5W, 5W25V are less than co-25V5W catalyst. Nevertheless, no clear effect on the amount of Lewis acid site could be

observed in the presence and absence of W. Possibly, depend on loading sequence during the preparation of W promoted V_2O_5/TiO_2 catalysts.

Figure 5.38 shows the spectra of the pyridine adsorption over co-25V10W catalyst. From the spectra of co-25V5W and co-25V10W, it is found that both co-25V5W and co-25V10W show similar acid strength and amount of both Brønsted and Lewis acid sites. It is possible that 5 wt.% WO_3 is a limit the generation of Brønsted acid sites and Lewis acid sites.

When adding 1 wt.% of K on based catalyst, the acid strength of 25V1K is similar to 25V catalyst (figure 5.39). Regarding co-25V3K, both acid strength and amount of the catalyst seems to drop compare with the based catalyst (figure 5.40). This means that potassium lead to the reduction of surface acidity. However, 3K25V and 25V3K catalysts are the catalysts which can not detect their surface acidity. Possibly, the sequence of K loading has some effect on the system of catalysts and consequently detection of surface acidity. Figure 5.41 shows the spectra of the pyridine adsorption over co-25V5K catalyst. This catalyst has the acid strength less than co-25V3K catalyst.

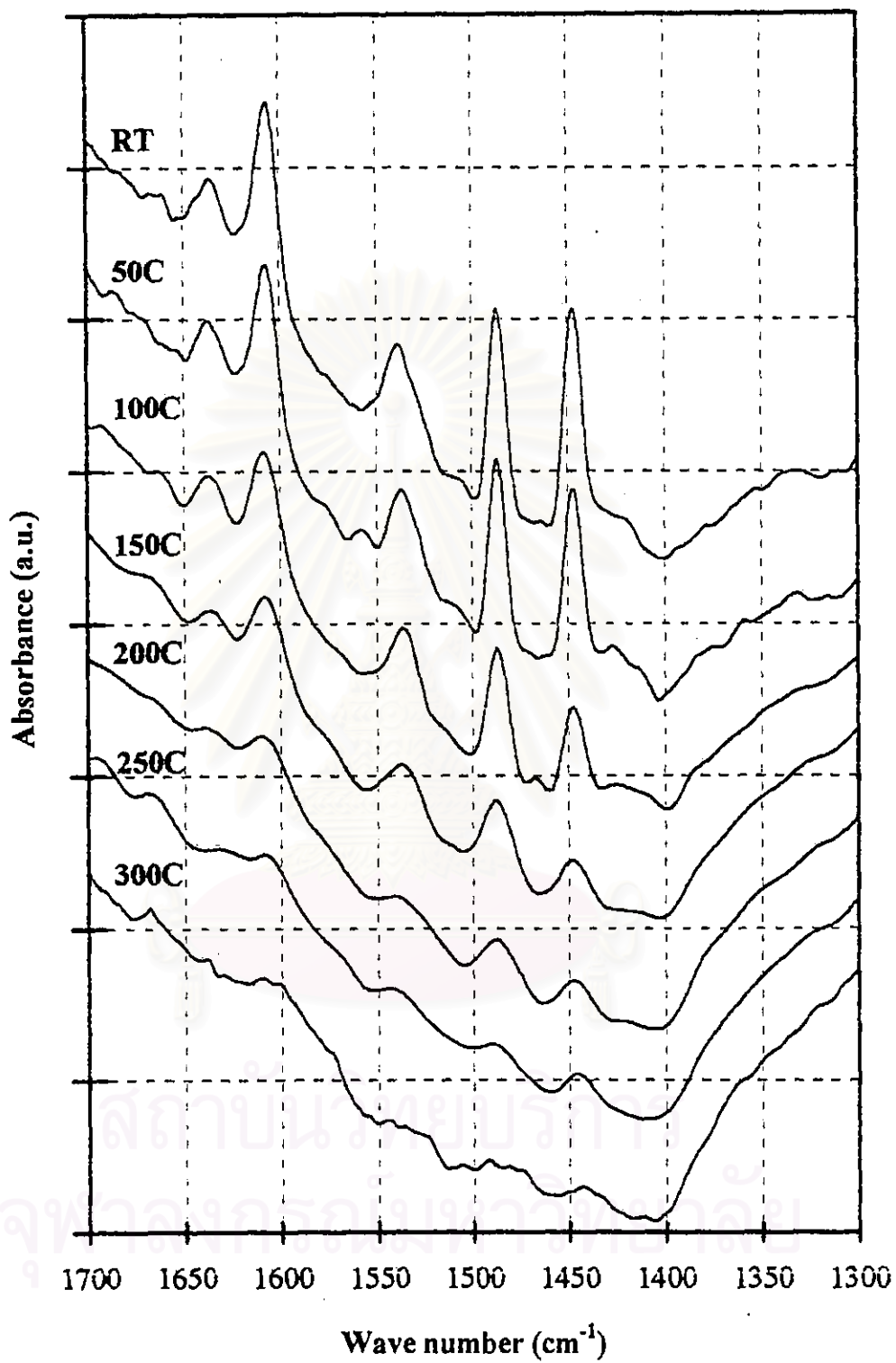


Figure 5.33: Pyridine adsorption of 25V catalyst

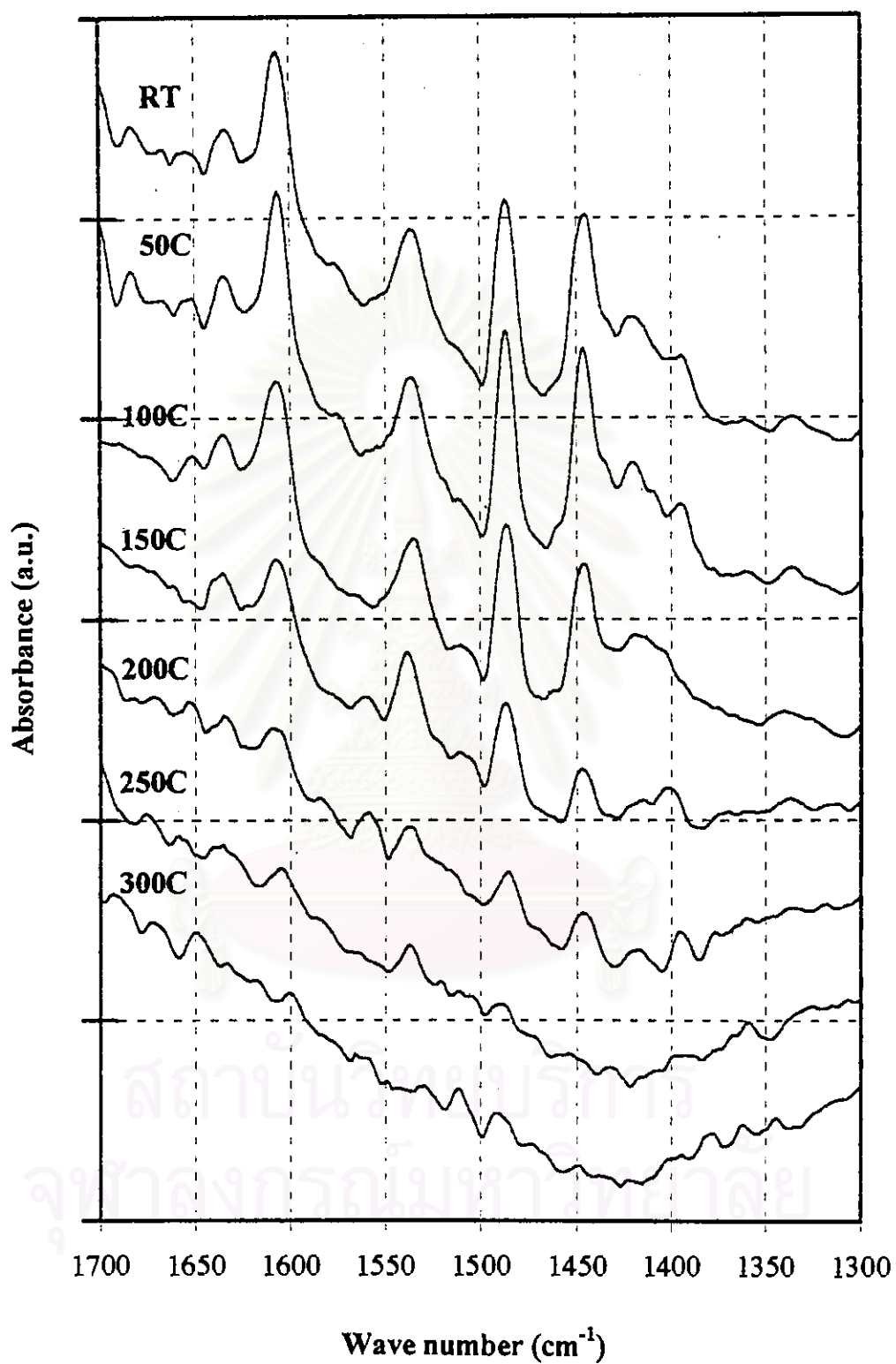


Figure 5.34: Pyridine adsorption of co-25V₂W catalyst

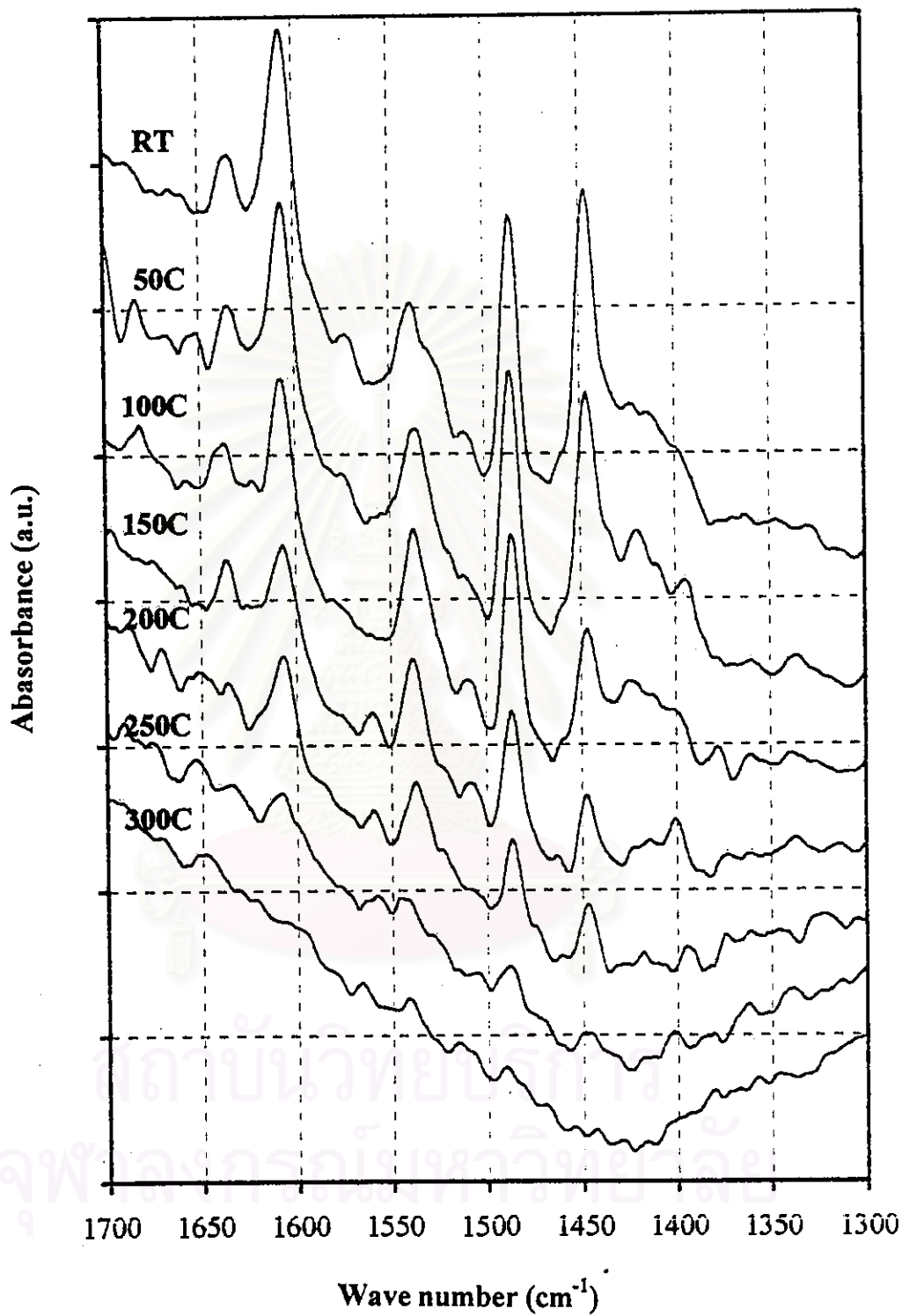


Figure 5.35: Pyridine adsorption of co-25V5W catalyst

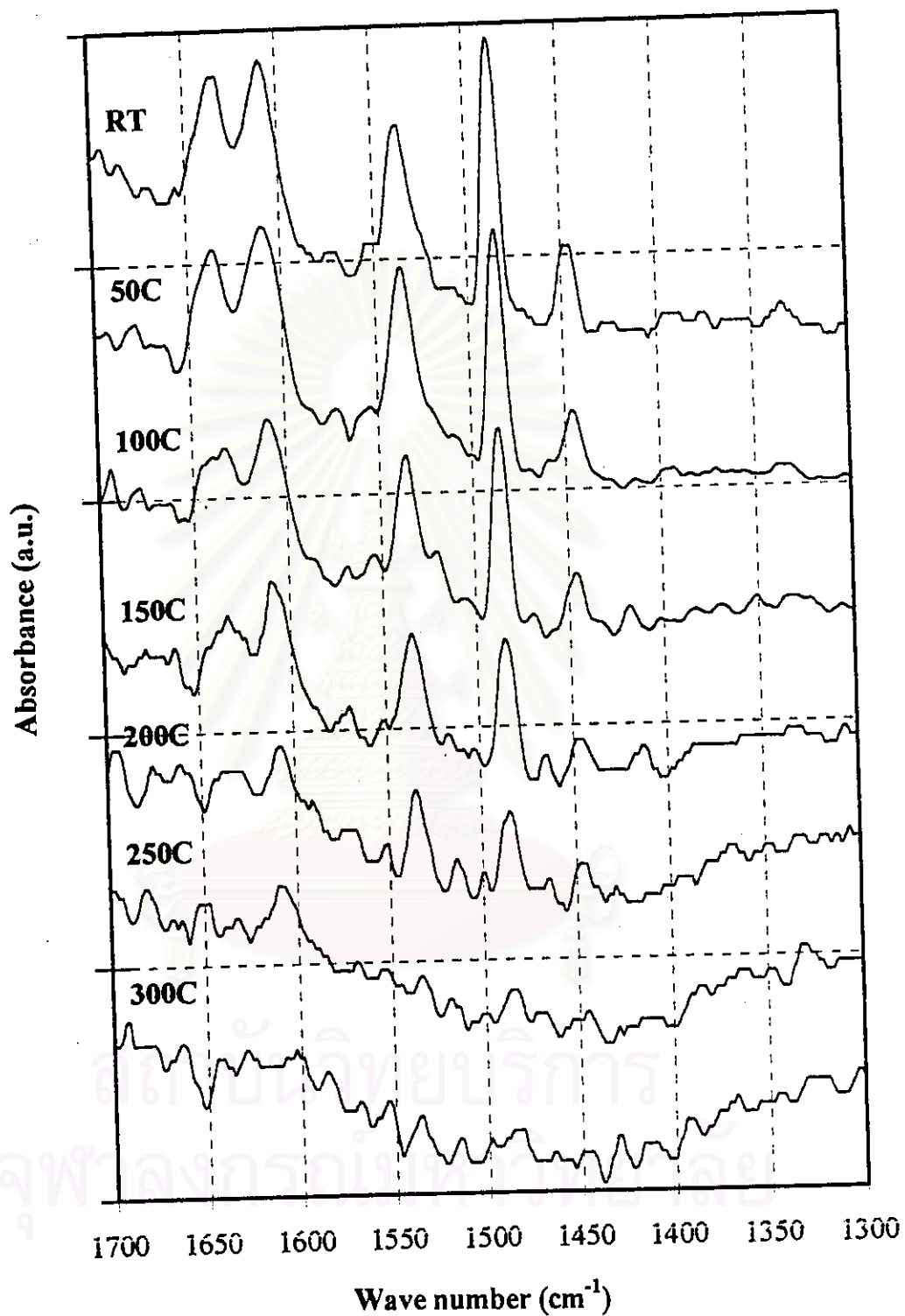


Figure 5.36: Pyridine adsorption of 25V5W catalyst

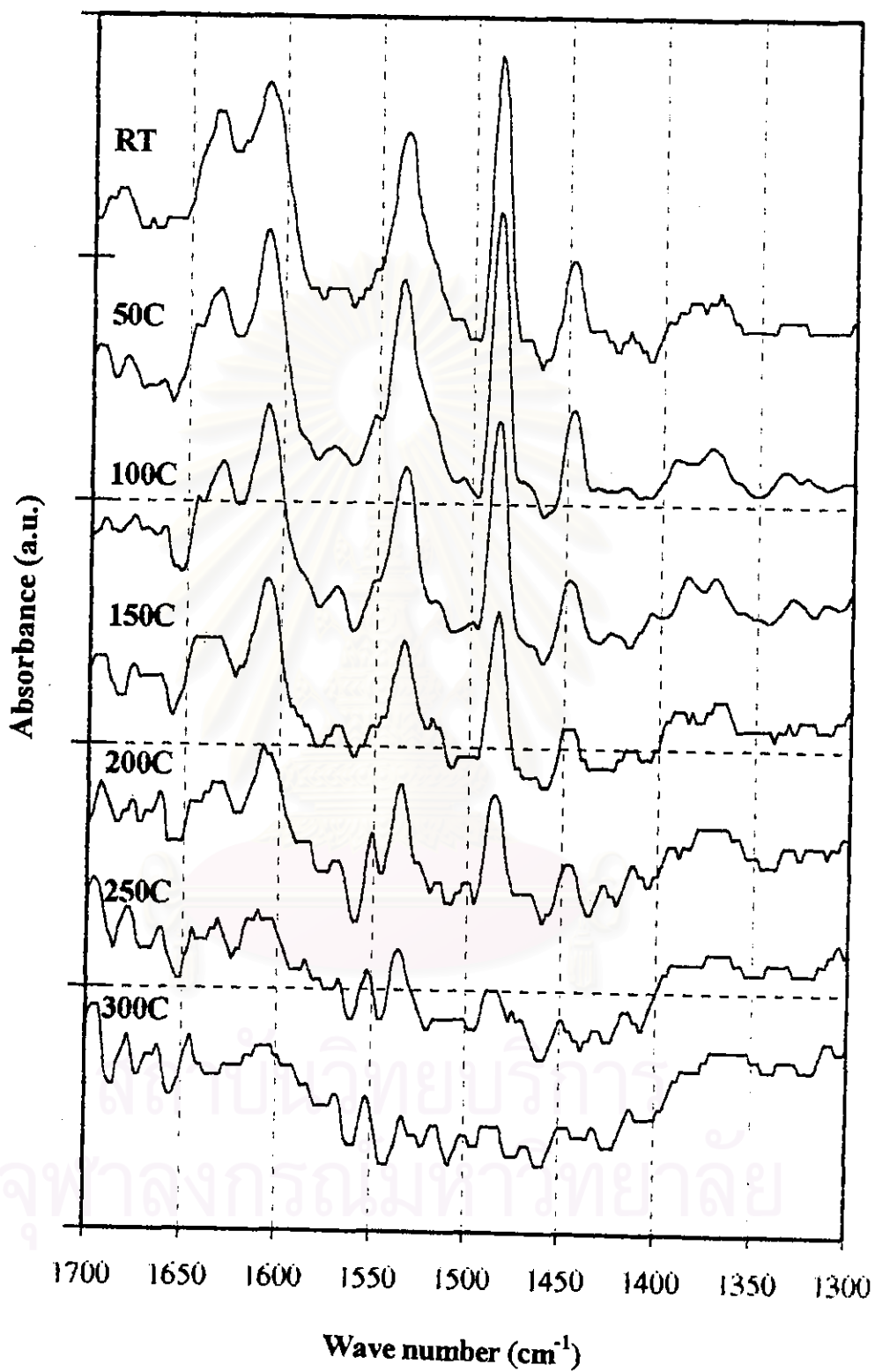


Figure 5.37: Pyridine adsorption of 5W25V catalyst

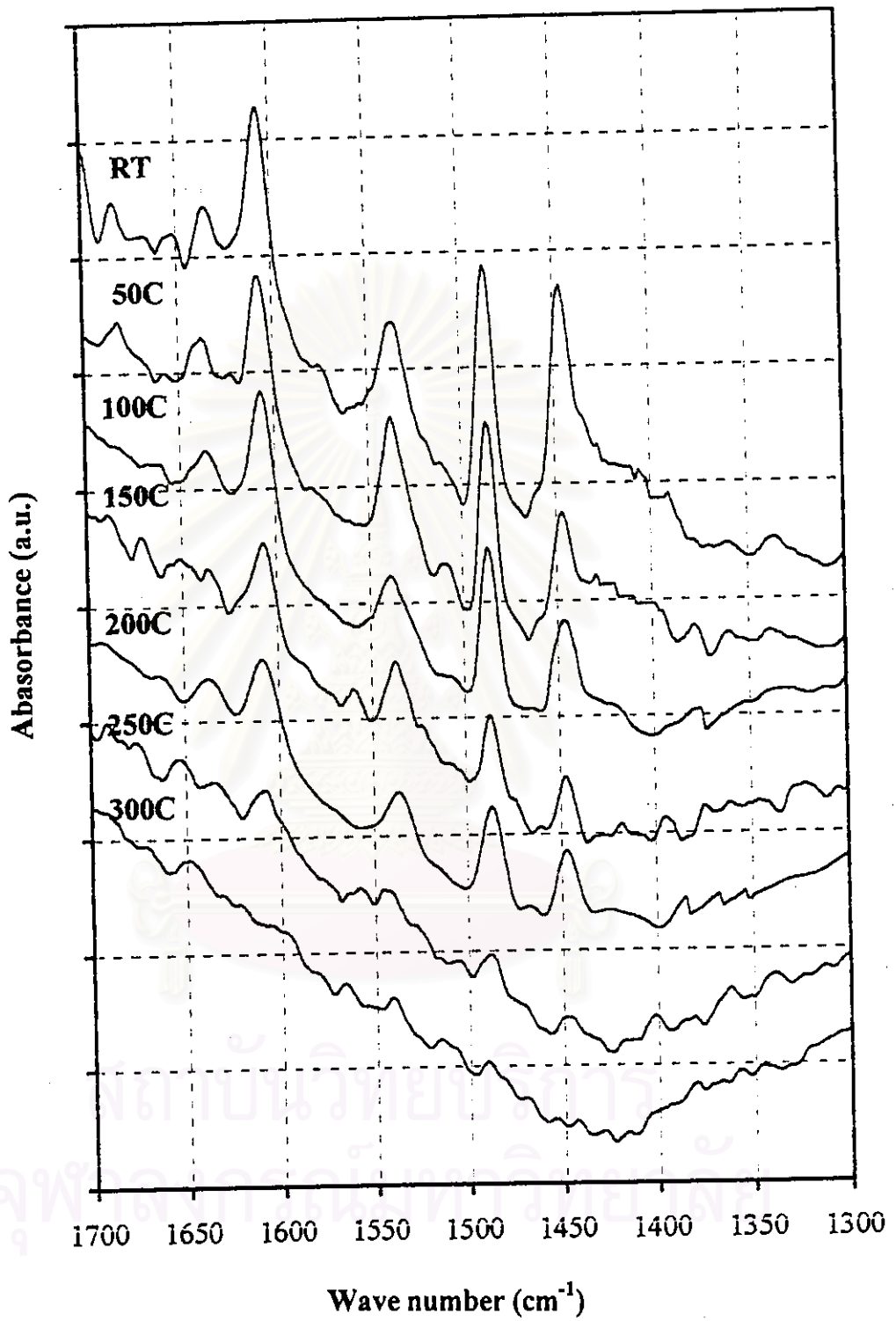


Figure 5.38: Pyridine adsorption of co-25V10W catalyst

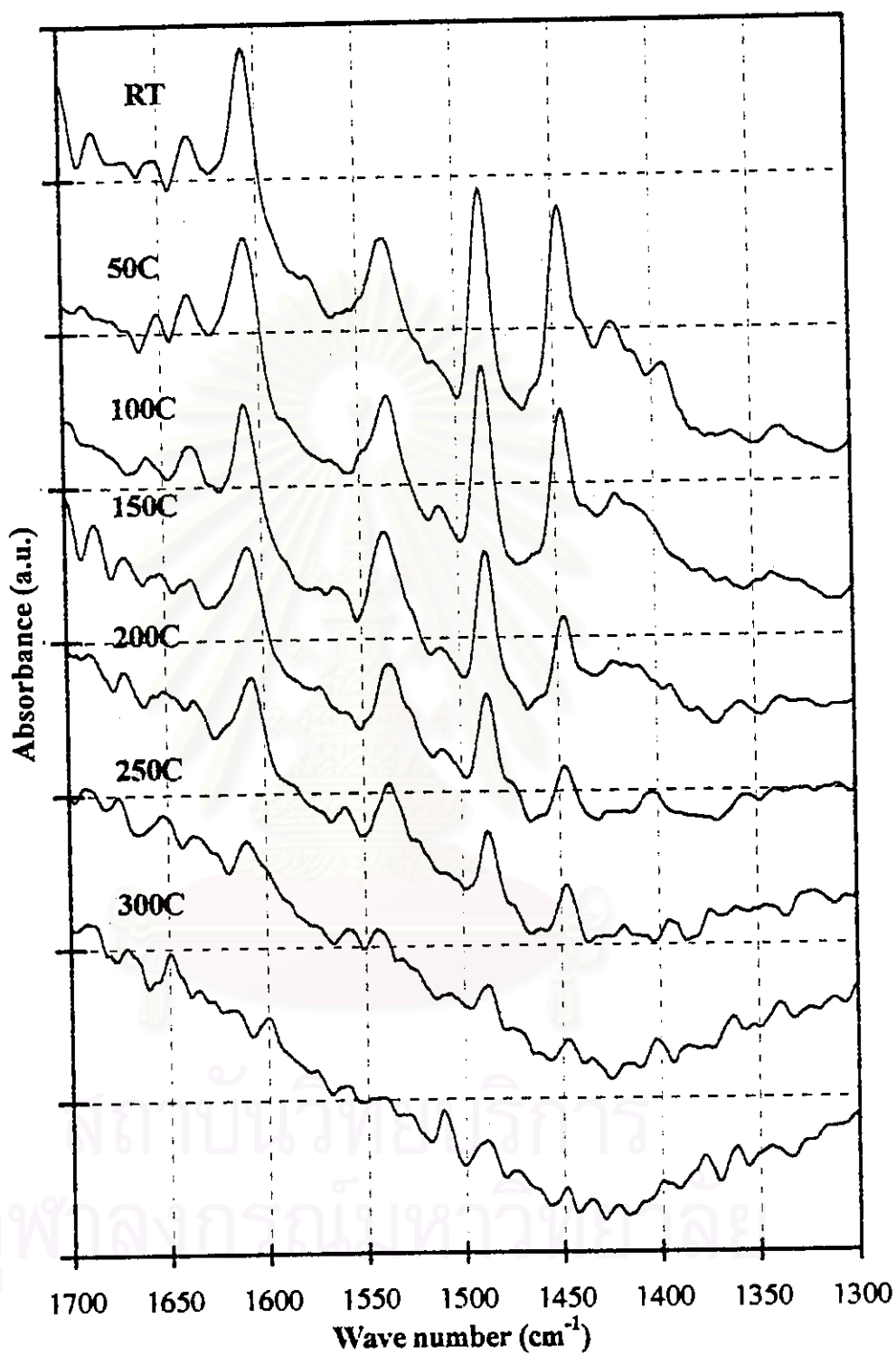


Figure 5.39: Pyridine adsorption of co-25V1K catalyst

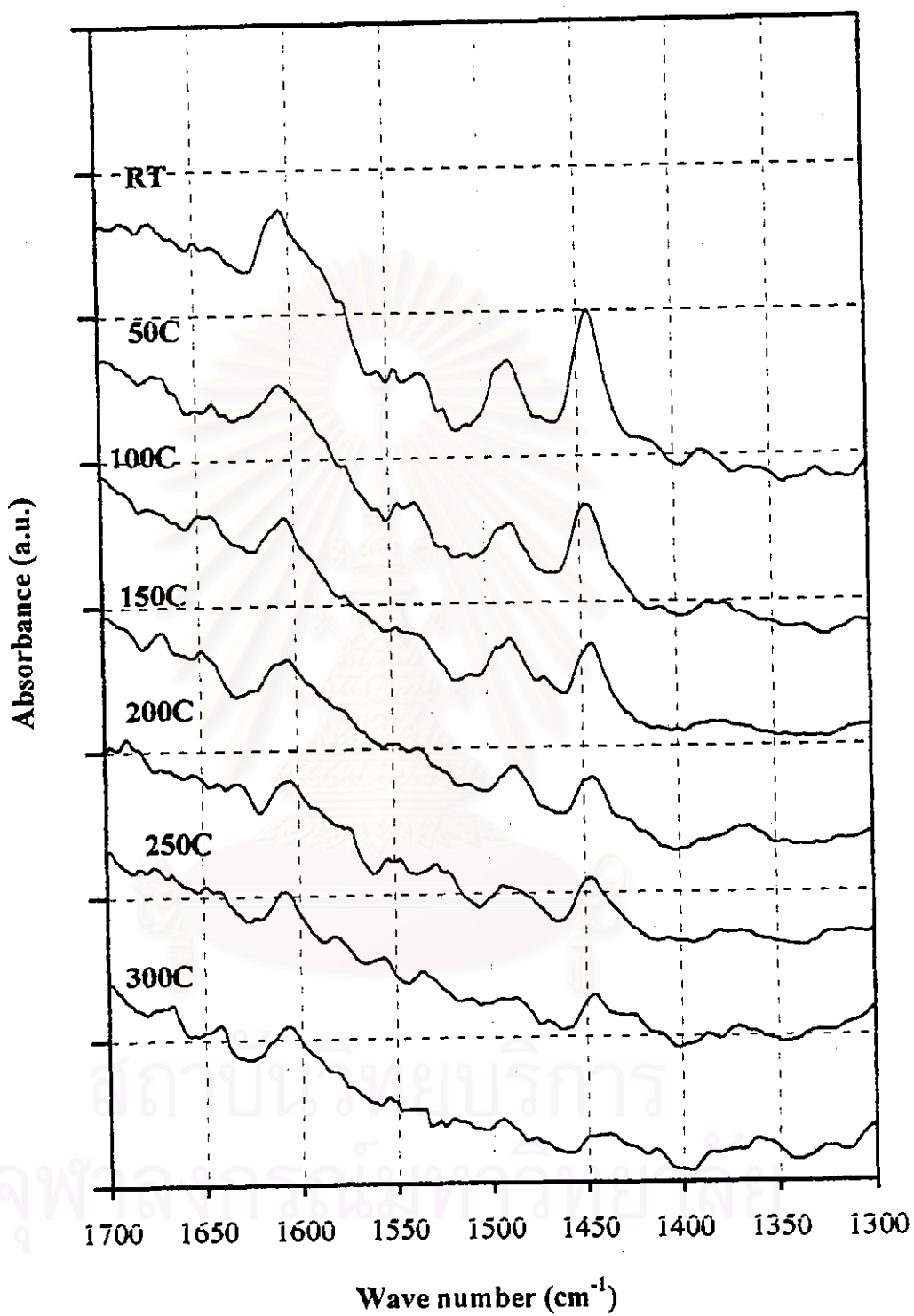


Figure 5.40: Pyridine adsorption of co-25V3K catalyst

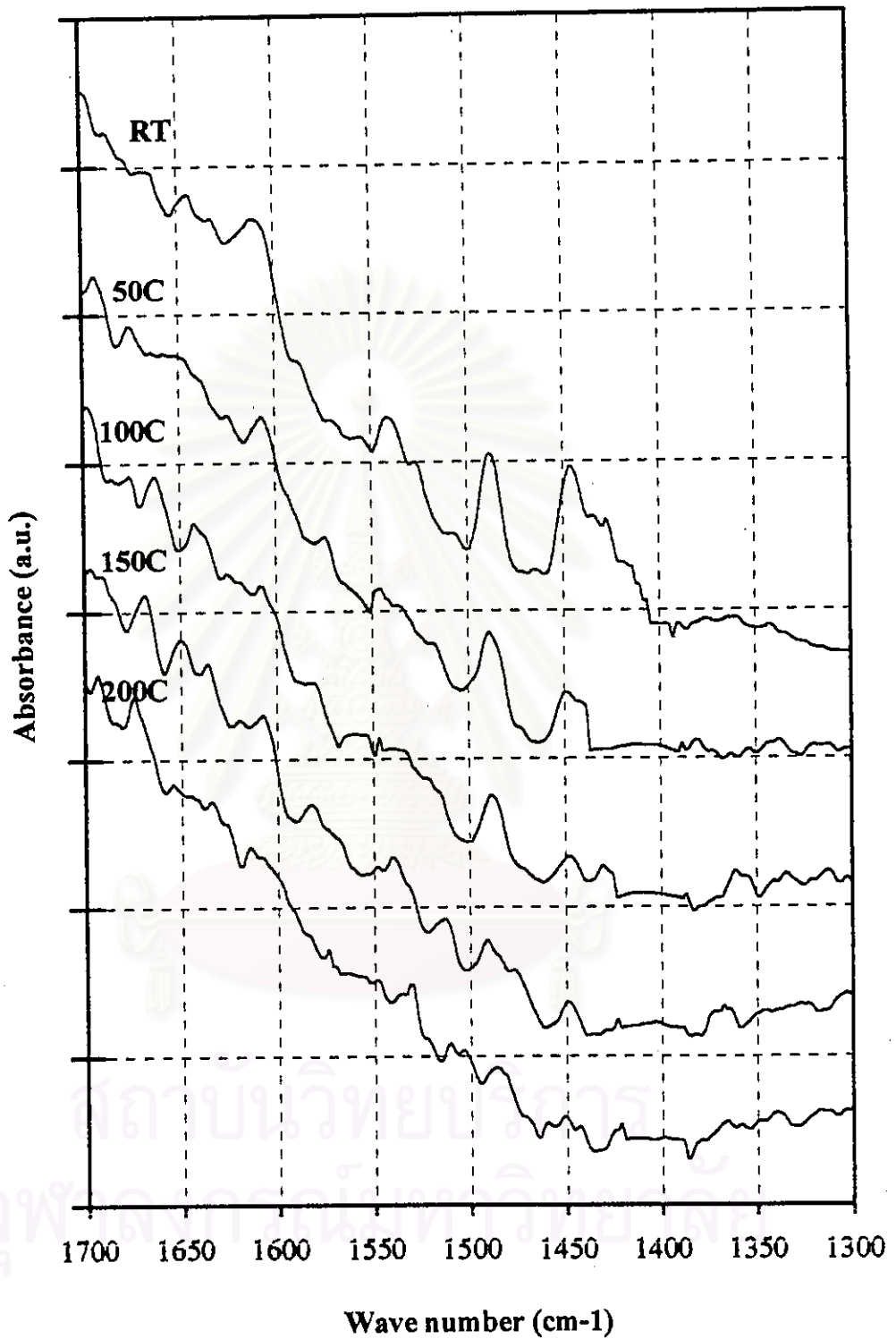


Figure 5.41: Pyridine adsorption of co-25V5K catalyst

5.4 Effect of tungsten and potassium loading added on V_2O_5/TiO_2 catalysts

This section investigates the effect of W and K loading over 25V based catalyst for the reduction of NO_x . The experiment was performed in the temperature range of 50 to 500°C which the reactant gas feed concentration was kept constant at 500 ppm NO, 500 ppm NH_3 , 2 vol.% O_2 , 50 ppm SO_2 and 10 vol.% H_2O , respectively. These conditions are the typical values in flue gases of power plants. [Lintz & Turek (1992)]

Figure 5.42 represents the comparison between SCR activity versus WO_3 loading on based catalyst. The SCR activity of 25V increases with increasing reaction temperature until the maximum NO conversion is reached at temperature 300°C and before decreasing at higher reaction temperature. This decrease is caused by the direct oxidation of ammonia to nitric oxide which is an undesired side reaction. This side reaction becomes significant only at high temperature (above 350°C). The result of ammonia oxidation reaction is shown in section 5.6.

When 2 wt.% WO_3 was added to the base catalyst, the behavior of co-25V2W catalyst is still similar to 25V catalyst at temperature below 300°C. The maximum NO conversion is reached (about 70 %) at temperature around 300°C before continuously decreases. In the case of co-25V5W catalyst, the relationship between NO conversion and reaction temperature is similar to co-25V2W catalyst, but with 20-50 % higher in NO conversion.

When WO_3 loading was increased up to 10 wt.%, it was found that NO conversion increases with reaction temperature until reaching a maximum at reaction temperature about 350°C (about 70%) and then decreases. When compare to 5 wt.% WO_3 loading, it can be observed that the activity of 10 wt.% WO_3 loading is less active. The lower conversion of 25V10W is due to too high amount of WO_3 loading. It is associated with BET surface area and IR spectra of catalyst (table 5.1, figure 5.26).

The comparison between NO conversion versus K_2O loading on 25V catalyst is depicted in figure 5.43. Co-25V1K catalyst has similar behavior with 25V catalyst; however, the NO conversion of co-25V1K catalyst shows a better performance than 25V catalyst at higher temperature. The SCR activity of co-25V3K catalyst is similar to co-25V1K catalyst but slightly less active. It was found that NO conversion increases with increasing reaction temperature until the maximum NO conversion is reached (about 70 %) at temperature around 350°C before continuously decreases.

Addition of K_2O loading up to 5 wt.%, the behavior of this catalyst is not like the previous catalysts. This catalyst showed a good performance below 250°C (higher than base catalyst). On the contrary, above 250°C , the NO conversion of the catalyst is less than the base catalyst, also co-25V1K, co-25V3K catalysts. It is possible that some new compounds are formed on co-25V5K catalyst which can change the performance of the catalyst.

Eventually, the experiments on effect of tungsten and potassium loading have pointed out that 5 wt.% WO_3 is the optimum loading on the based catalyst due to highest in NO conversion, and 3 wt.% K_2O loaded on the based catalyst is the minimum requirement to see any change in NO conversion.

สถาบันวิทยบริการ
จุฬาลงกรณ์มหาวิทยาลัย

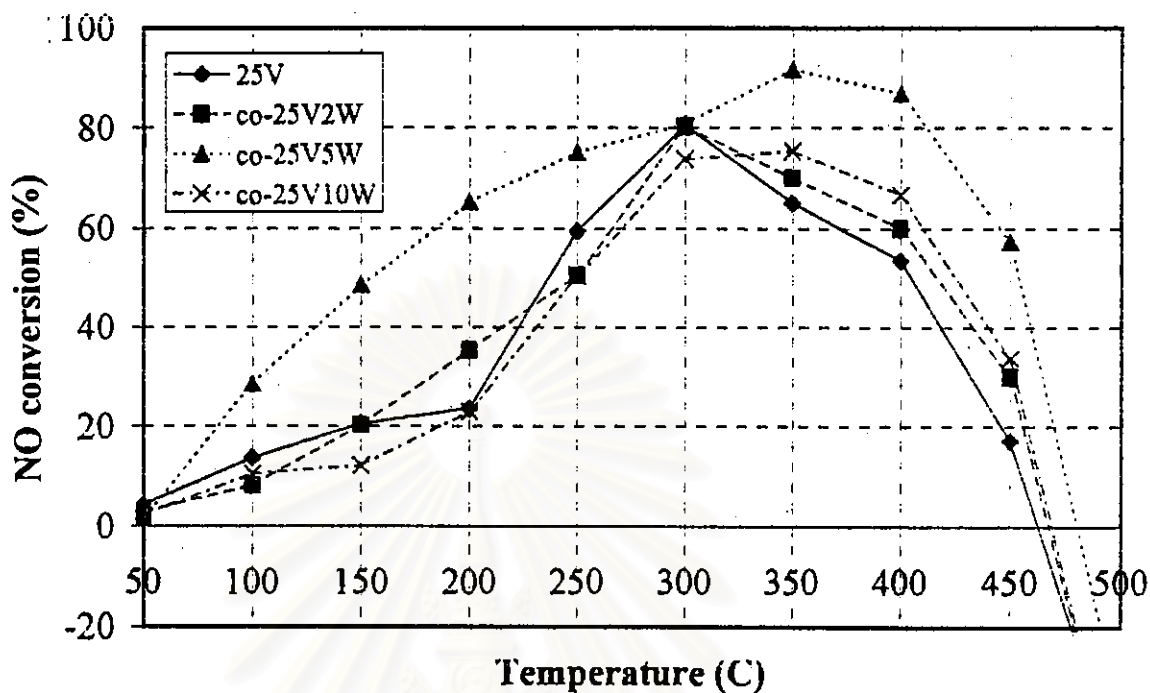


Figure 5.42: SCR activity versus WO_3 loading on based catalyst

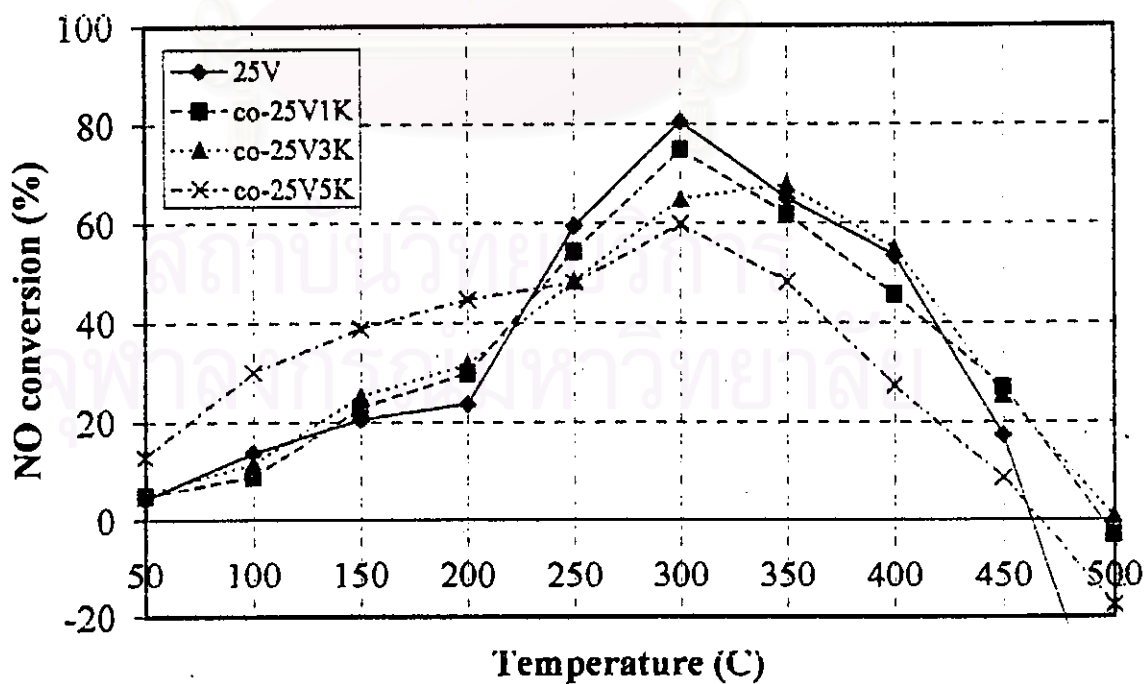


Figure 5.43: SCR activity versus K_2O loading on based catalyst

5.5 Effect of loading sequence of tungsten and potassium added on V_2O_5/TiO_2 catalysts

From the results of section 5.4, it can be concluded that 5 wt.% WO_3 - 25 wt.% V_2O_5 is the optimum catalyst. And 3 wt.% K_2O - 25 wt.% V_2O_5 is the interested catalyst because this loading can see the difference in NO conversion. Therefore, 5 wt.% WO_3 - 25 wt.% and 3 wt.% K_2O - 25 wt.% V_2O_5 catalysts are further studied. This section demonstrates the effect of loading sequence during the preparation of a W promoted on V_2O_5/TiO_2 catalyst (25 wt.% V_2O_5 , 5 wt.% WO_3) and K added on V_2O_5/TiO_2 catalyst (25 wt.% V_2O_5 , 3 wt.% K_2O). The conditions of testing are the same as in section 5.4. In addition, the catalysts in this section are compared with the based catalyst (25V) too.

The behavior of the ternary catalysts (tungsten added) are similar to that of the binary catalyst. For co-25V5W catalyst, the NO conversion could reached about 90% at temperature around $350^\circ C$ while the NO conversion of 25V5W and 5W25V catalysts level off at 70-75 % at reaction temperature $300-350^\circ C$. At high reaction temperature, a significant drop in NO conversion is observed, due to the result of NH_3 oxidation as in the binary catalyst occurs. [Kanongchaiyot *et al.* (1998)] Figure 5.44 exhibits the comparison of catalytic activity for the SCR reaction on 25V, 25V5W, 5W25V and co-25V5W catalysts.

A significant difference among the NO conversion of the binary catalyst and the ternary catalysts can be explained using changes in acidity of the catalyst surface. Co-25V5W catalyst shows higher amount of Lewis acid site than 25V5W, 5W25V and the base catalyst (figures 5.33, 5.35 – 5.37). While the ternary catalysts show the same amount of Brønsted acid whereas difference on activity. In addition, the amount of Lewis acid can be used to explain the difference on activity. The amount of Lewis acid site on 25V5W, 5W25V are less than co-25V5W, therefore, the activity of 25V5W, 5W25V are less than co-25V5W. However, this result can not suggest that Brønsted acid site does not completely involve in the SCR reaction.

The formation of the species is a possible reason that can change the Lewis acid site when change the loading sequences. Co-25V5W catalyst may form the complex of $W_xV_yO_z$ while 25V5W and 5W25V catalysts may form WO_3 and V_2O_5 on the catalyst surface. Nevertheless, the complex oxide is formed on co-loading method can not observed by XRD measurement.

The behavior of the ternary catalysts (potassium added) are similar to that of the binary catalyst. 3K25V catalyst shows higher conversion than 25V3K catalyst. However, the NO conversion of both 3K25V and 25V3K are less than co-25V3K catalyst. The different performance of the three type of 3 wt.% K_2O - 25 wt.% V_2O_5 can be explained by differences in the species which are formed on the catalysts. [Courcot *et al.* (1997)] The species of the three type of 3 wt.% K_2O - 25 wt.% V_2O_5 are shown in figures 5.28 – 5.30. The comparison of NO conversion versus loading sequence of potassium is disclosed in figure 5.45.

Finally, it can be concluded that the loading sequence of both W and K introduced over V_2O_5/TiO_2 catalysts have some effect on the catalytic activity of the catalyst. Co-loading method shows the highest activity compared with other methods.

สถาบันวิทยบริการ
จุฬาลงกรณ์มหาวิทยาลัย

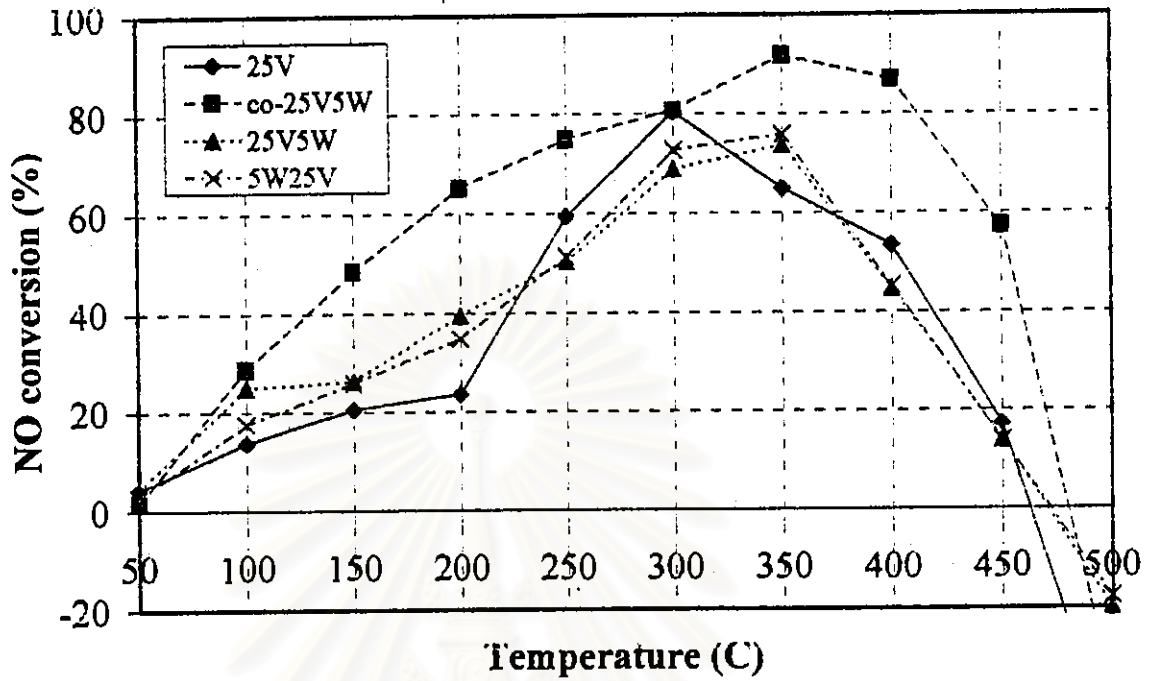


Figure 5.44: SCR activity versus loading sequence of W

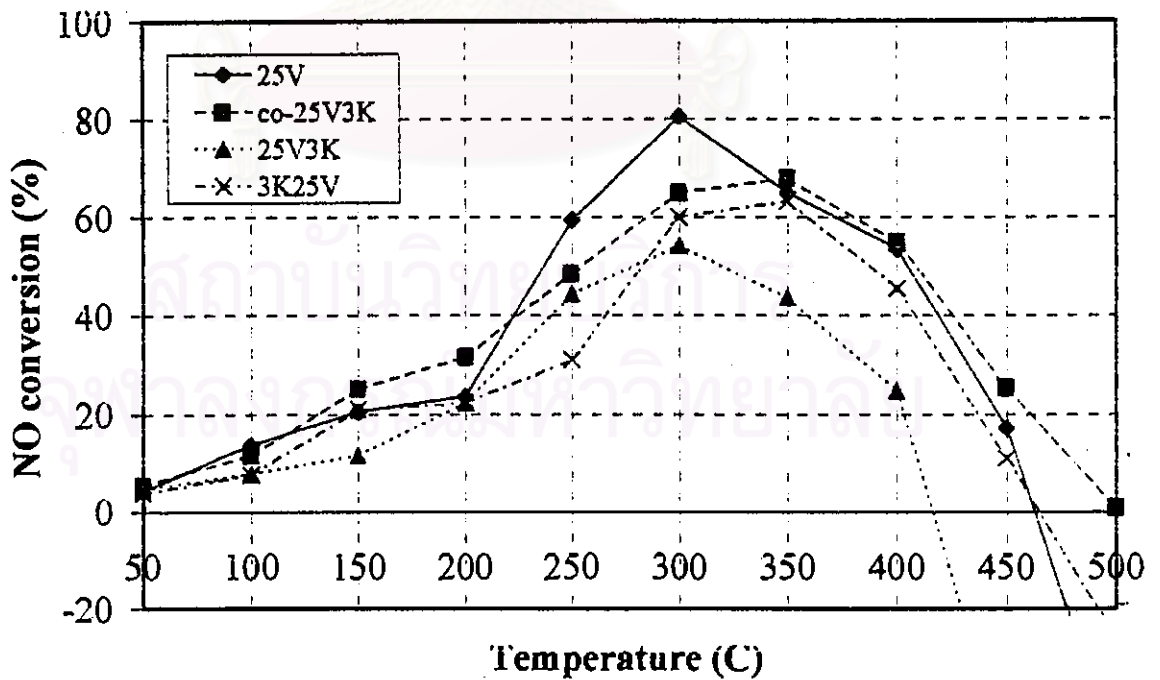


Figure 5.45: SCR activity versus loading sequence of K

5.6 Role of tungsten and potassium on the catalysts

This section discusses role of tungsten and potassium on the catalysts. Figures 5.46 – 5.50 depict the comparison among the interested catalysts (25V, co-25V5W, co-25V3K and 25V5W3K) with the SCR activity in several conditions (*i.e.* NO+NH₃, NO+NH₃+O₂, NO+NH₃+O₂+SO₂, NO+NH₃+O₂+H₂O and NO+NH₃+O₂+SO₂+H₂O conditions). From the results, co-25V5W catalyst shows the highest NO conversion compared with 25V and co-25V3K catalysts at lower temperature. At higher temperature (above 300-350°C), trends of the NO conversion are opposite to at lower temperature.

The different in NO conversion can be explained using changes in acidity of the catalyst surface (figures 5.33, 5.35, 5.40). A significant difference in acidity among 25V, co-25V5W and co-25V3K is co-25V5W shows the highest Lewis acidity as well as both acid strength and amount. This result accompany with the highest NO conversion of co-25V5W catalyst suggests that the Lewis acid site is likely to be an active center in the SCR mechanism more than Brønsted acid site. Nevertheless, increasing in acidity has some negative effects. In the high reaction temperature region (above 300°C), the decrease in NO conversion is in the following order: co-25V5W > 25V > co-25V3K. This order is also in the same sequence as the Brønsted and Lewis acidity: co-25V5W > 25V > co-25V3K. Thus, it can be suggested that in the high reaction temperature region the oxidation of NH₃ to nitrogen oxides by the amount of Lewis acidity is more pronounced than the SCR path. This explanation can be related to the ammonia oxidation reaction. The generation of NO in ammonia oxidation reaction is in the following order: co-25V5W > 25V > co-25V3K. Figures 5.51, 5.52 show the ammonia oxidation of these catalysts in the presence and absence of SO₂ and water (NH₃+O₂, NH₃+O₂+SO₂+H₂O).

Moreover, some literatures proposed a reason for the role of tungsten that can enhance the SCR activity. [Alemany *et al.* (1995), Lietti *et al.* (1996a, b, c)] They claimed that there was an existence of a specific synergism in the SCR reaction between V and W in the ternary catalyst. This synergism could be related to the

strong electronic interactions that exist between V and W surface species and the TiO_2 support, which led to the reducibility higher catalyst. Thus, it can be pointed to the superior redox properties of the co-25V5W catalyst with respect to the based catalyst. However, the catalyst which additional potassium has not ever been investigated in their literatures.

In other words, tungsten increases the acid property (both strength and amount) on the catalyst surface. Consequently, enhances the activity in SCR reaction at lower temperature including accelerates the ammonia oxidation reaction at higher temperature too. In contrast, potassium decreases the acid property (both strength and amount) on catalyst surface. Therefore, the activity of the catalyst that added potassium is dropped at lower temperature. However, potassium can inhibit the oxidation of ammonia at higher temperature. This is an advantage of potassium which is contained in the catalyst.

Anyway, the 25V5W3K catalyst has activity in between the activity of 25V and co-25V3K catalysts. This result indicates that the addition of W can increase the resistance to alkaline metal deactivation.

สถาบันวิทยบริการ
จุฬาลงกรณ์มหาวิทยาลัย

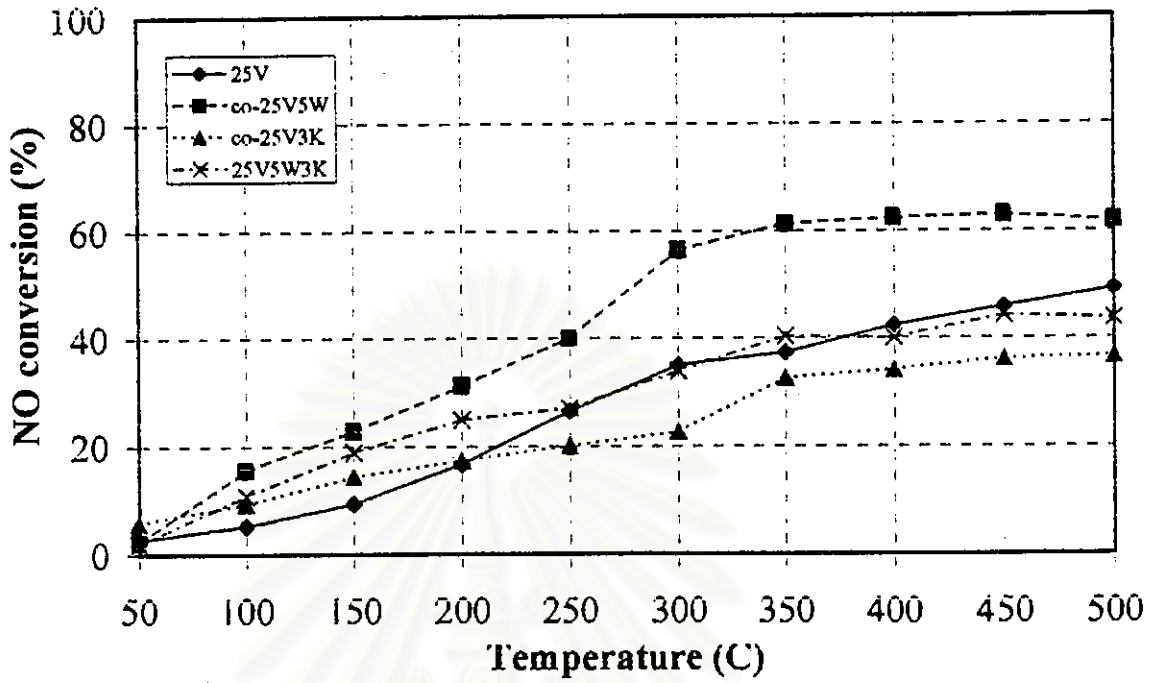


Figure 5.46: SCR activity of catalysts under $\text{NO}+\text{NH}_3$ atmosphere

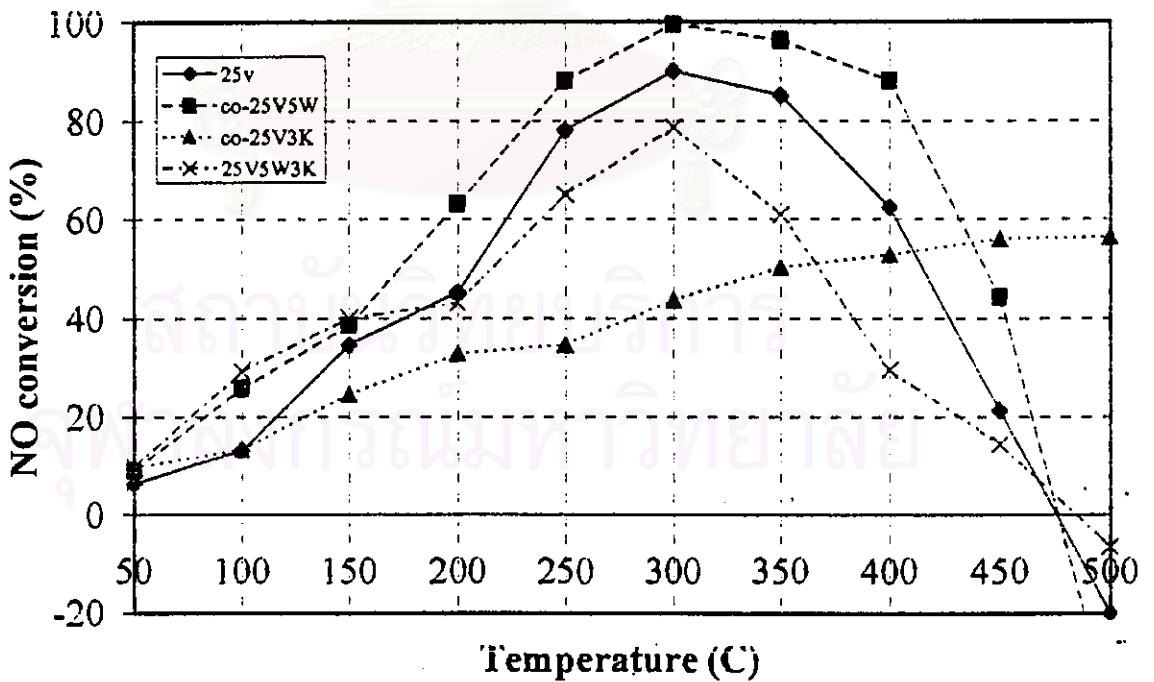


Figure 5.47: SCR activity of catalysts under $\text{NO}+\text{NH}_3+\text{O}_2$ atmosphere

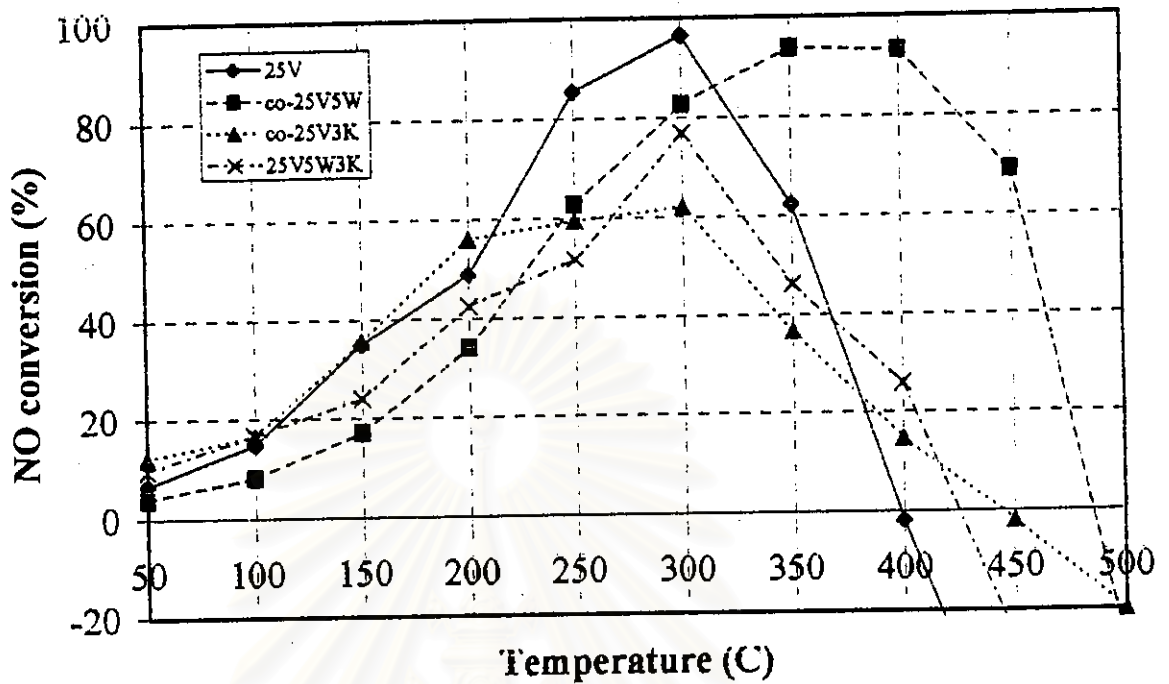


Figure 5.48: SCR activity of catalysts under $\text{NO} + \text{NH}_3 + \text{O}_2 + \text{SO}_2$ atmosphere

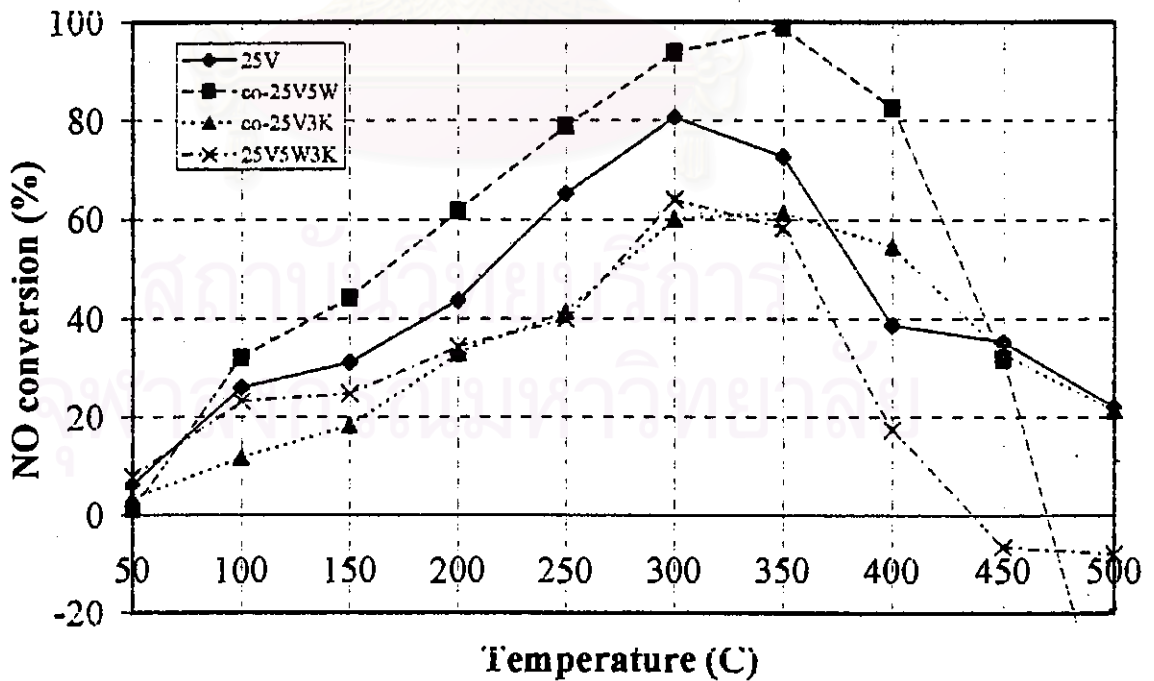


Figure 5.49: SCR activity of catalysts under $\text{NO} + \text{NH}_3 + \text{O}_2 + \text{H}_2\text{O}$ atmosphere

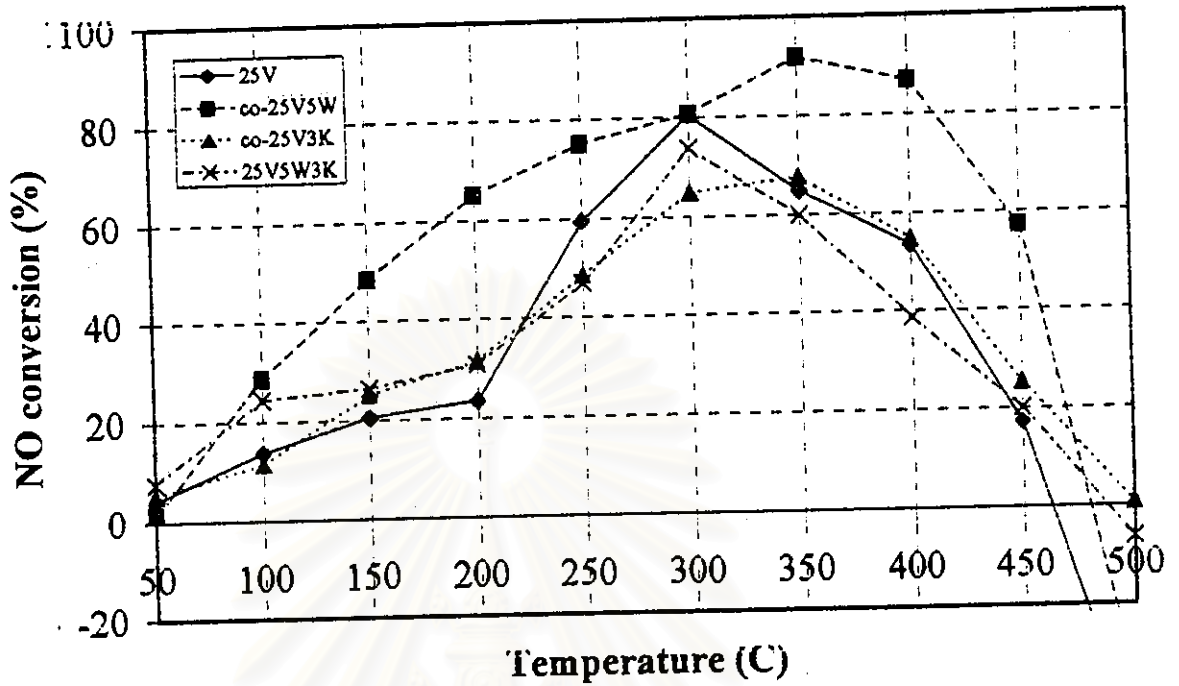


Figure 5.50: SCR activity of catalysts under NO+NH₃+O₂+SO₂+H₂O atmosphere

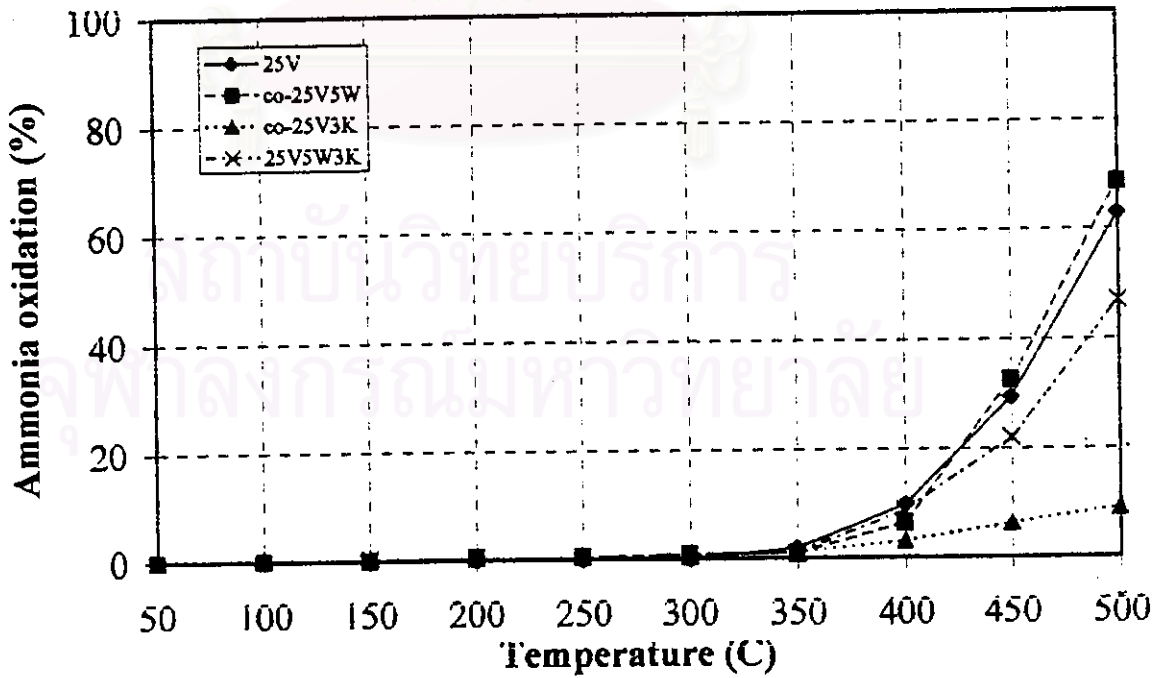


Figure 5.51: SCR activity of catalysts under NH₃+O₂ atmosphere

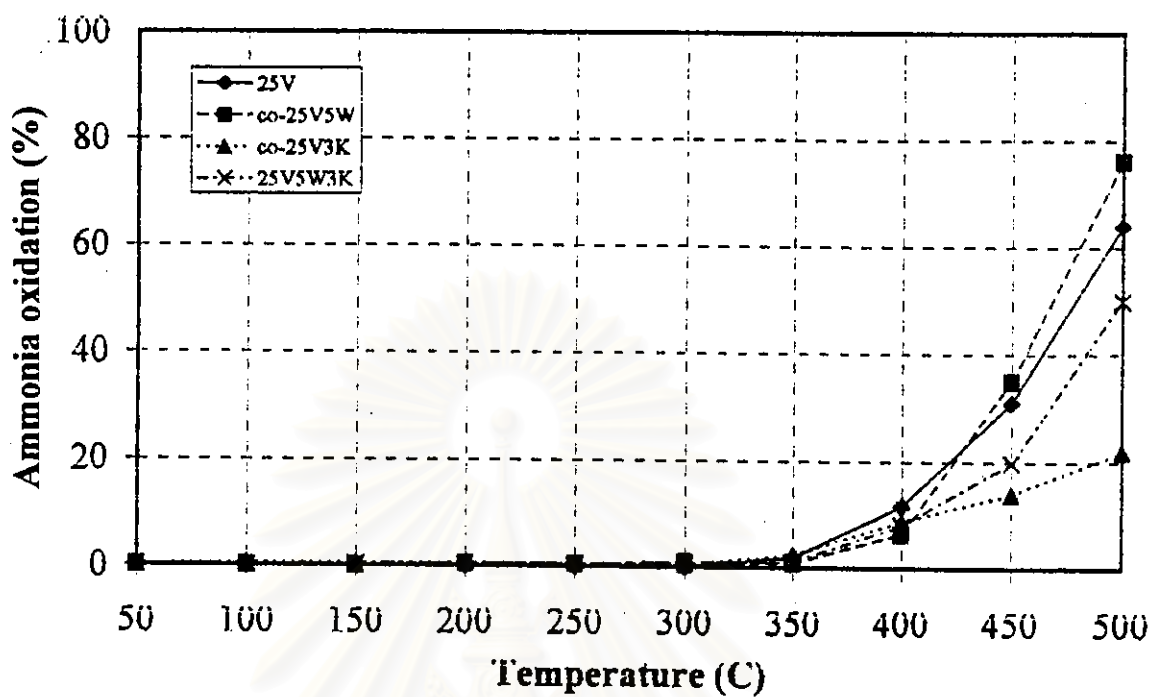


Figure 5.52: SCR activity of catalysts under $\text{NH}_3+\text{O}_2+\text{SO}_2+\text{H}_2\text{O}$ atmosphere

สถาบันวิทยบริการ
จุฬาลงกรณ์มหาวิทยาลัย

5.7 The catalytic behavior of the catalysts

5.7.1 Base catalyst (25V)

The catalytic behavior of 25V catalyst under operating condition of several reactant gases, NO+NH₃, NO+NH₃+O₂, NO+NH₃+O₂+SO₂, NO+NH₃+O₂+H₂O, NO+NH₃+O₂+SO₂+H₂O, NH₃+O₂ and NH₃+O₂+SO₂+H₂O were further investigated. Figure 5.53 shows the SCR activity versus reaction temperature under NO+NH₃, NO+NH₃+O₂, NO+NH₃+O₂+SO₂, NO+NH₃+O₂+H₂O and NO+NH₃+O₂+SO₂+H₂O conditions. The NO self-decomposition and NO oxidation are found to be negligible because the NO conversion of NO decomposition and NO oxidation slightly changes when compare to the previous reactions. And the formation of reaction product was slightly observed during blank experiments, the influence of homogeneous uncatalyzed gas-phase reaction is negligible. [Teratrakoonwicha (1996)] Preliminary study was also performed in the reaction temperature range of 50-500°C.

In the case of NO+NH₃ condition, the NO conversion progressively increases with increasing reaction temperature. When O₂ was added, the NO conversion rapidly increases with increasing temperature until the maximum NO conversion is reached at reaction temperature about 300-350°C. At reaction temperature beyond 350°C, the NO conversion begin to drop as the result of ammonia oxidation to nitrogen oxide which is an undesired side reaction. The mechanism for the reaction of NO and ammonia over low loaded V₂O₅/TiO₂ catalysts in the presence of oxygen is explored by several literatures. [Ramis *et al.* (1990), Ozkan *et al.* (1995), Topsøe *et al.* (1995a, b)] In brief, they postulated the following mechanism to explain this phenomenon. Ammonia adsorbed on the active sites. V=O groups are also involved in the reaction, and specifically in the activation of the adsorbed ammonia. This activation process involves the transfer or partial transfer of hydrogen from the NH₃ molecule and accordingly reduced V-OH sites and produced. Once ammonia has been activated, NO from the gas-phase reacts with the activated ammonia complex leading to the formation of an intermediate that then decompose to nitrogen and water. Regeneration of the active sites (*i.e.* oxidation of the reduced V⁴⁺-OH site to V⁵⁺=O

groups) occurs by gas-phase oxygen. So that oxygen enhances the rate of the SCR reaction by increasing the rate of the catalyst reoxidation. [Lietti *et al.* 1996c]] Another possible mechanism, oxygen accelerates the formation of intermediate. The SCR reaction occurs by a redox mechanism and via an amide intermediate. From the mentioned possible mechanisms, the role of oxygen can not be surely concluded nowadays. However, we can use some proposed mechanisms of low loaded V_2O_5/TiO_2 system to explain the results of high loaded V_2O_5/TiO_2 catalyst under SCR reaction conditions.

In condition of ammonia oxidation reactions (NH_3+O_2 , $NH_3+O_2+SO_2+H_2O$), NO begin to form on 25V catalyst at $350^\circ C$ and further progressively increases with increasing temperature. The result shown in figure 5.54 indicates that $NO+NH_3+O_2$ condition for 25V catalyst can lead to the formation of NO due to the direct oxidation of ammonia at temperature above $350^\circ C$ which leads to the decrease of NO conversion.

The effect of SO_2 on the SCR activity of 25V catalyst could be clearly observed when SO_2 was added to the reactant gas. At reaction temperature below $300^\circ C$ SO_2 seems to have some promoting effect on the NO conversion. As for higher temperature, the NO conversion in this region rapidly dropped, indicating severe oxidation of NH_3 to nitrogen oxide especially when SO_2 was present. [Sintarako *et al.* (1998)] This result agrees with that reported in some literature [Weng & Lee (1993), Alemany *et al.* (1995), Kijlstra *et al.* (1996)] showing that sulphate addition during the preparation of a low loaded V_2O_5/TiO_2 catalyst or surface sulphate formation during the reaction can increase the SCR activity. In this case, SO_2 does not affect the deactivation caused by deposition of ammonium (bi) sulphates. Moreover, the amount of Lewis acid site is increased when SO_2 is added into gas mixture both lower and higher temperature. [Sintarako (1998)] From results can be suggested that Lewis acid site is the active center of both SCR and ammonia oxidation reaction.

In the present of 10 vol.% H_2O , added water seems not to have any effect on the catalytic activity significantly in the reaction temperature ranges of $50-200^\circ C$. For

the reaction temperature above 200°C the NO conversion in the presence of 10 vol.% H_2O is slightly lower than without H_2O . Conversely, the NO conversion in the presence of 10 vol.% H_2O is higher than without H_2O at higher temperature. This may be caused by a competitive adsorption of water on active sites for ammonia adsorption thus decreasing the rate of reaction. In the same way, the competitive adsorption causes a decisive increase of the selectivity at higher temperature. Because the undesired side reaction (ammonia oxidation) are strongly inhibited by water. [Odenbrand *et al.* (1991), Lintz & Turek (1992)]

In the case of addition of 50 ppm SO_2 and 10 vol.% H_2O , it is observed that the relationship between NO conversion and reaction temperature is similar to that of the case without water and SO_2 . But the case without water and SO_2 has higher activity than with water and SO_2 . This behavior may be caused by the effect of both water and SO_2 .



สถาบันวิทยบริการ
จุฬาลงกรณ์มหาวิทยาลัย

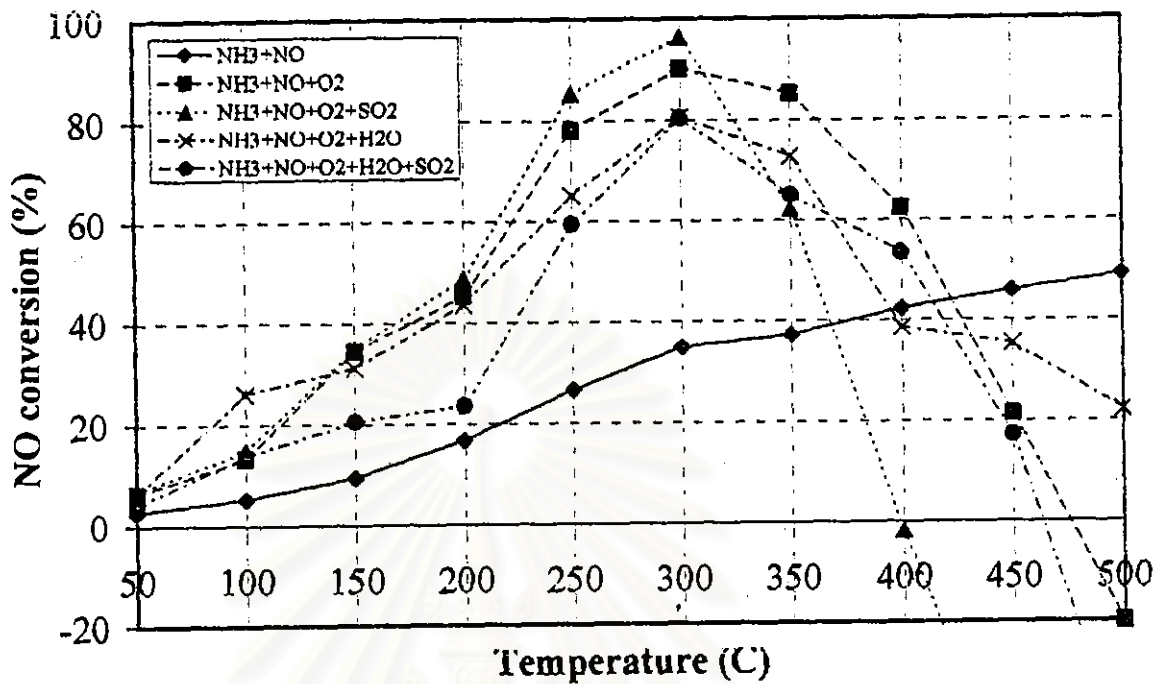


Figure 5.53: SCR activity of 25V catalyst under several operating atmospheres

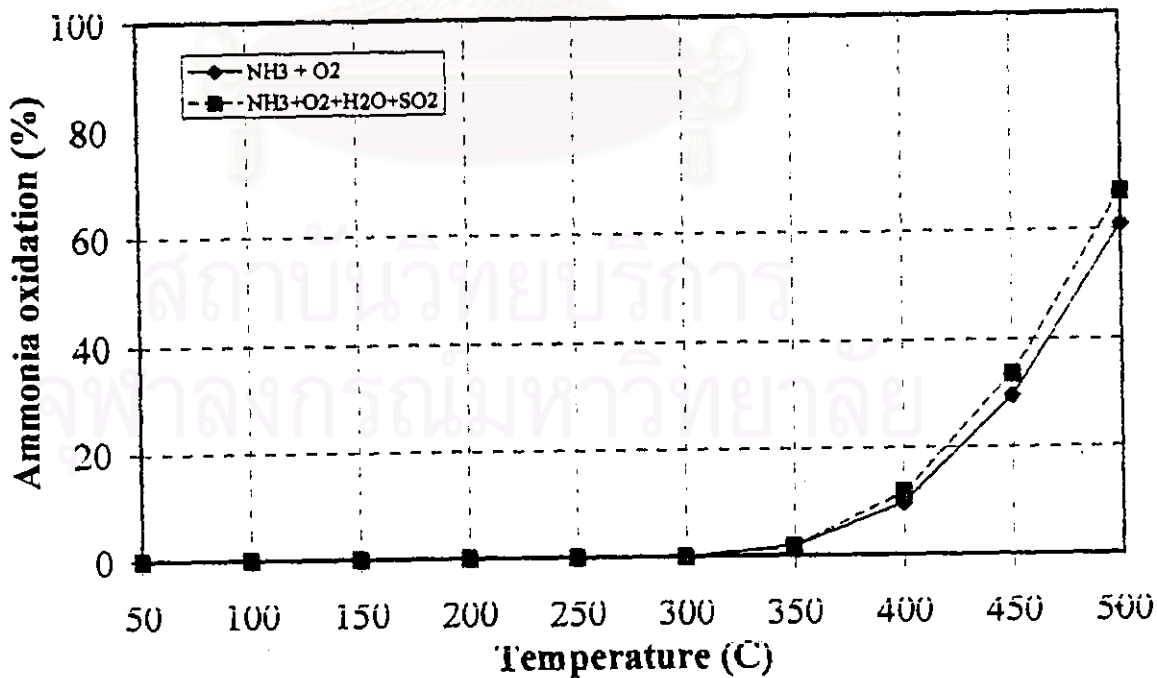


Figure 5.54: Ammonia oxidation reactions of 25V catalyst

5.7.2 *co-25V5W catalyst*

From the results of sections 5.4 and 5.5, *co-25V5W* is the best catalyst. Therefore, this catalyst is selected to explore its behavior in several reaction conditions. The operating conditions for investigation is still the same as of the based catalyst.

The experimental result shows that the behavior of *co-25V5W* is similar to that of 25V catalyst. Figure 5.55 shows the catalytic behavior of *co-25V5W* catalyst. In the case of $\text{NO} + \text{NH}_3 + \text{O}_2$ condition, the NO conversion of *co-25V5W* catalyst can reached 80-95 % at reaction temperature around 300°C and can maintain this conversion up to 400°C . A significant drop in NO conversion is observed when the reaction temperature is further increased up to 450°C . The decrease in NO conversion at high temperature is also the result of NH_3 oxidation as in the case of 25V catalyst.

In the case of ammonia oxidation reactions over *co-25V5W* catalyst, NO is formed over *co-25V5W* catalyst at 350°C and further progressively increases with increasing temperature. This reaction of *co-25V5W* catalyst liked 25V catalyst. The result is shown in figure 5.56.

The behavior after addition of 50 ppm SO_2 to the reacting gas mixture does not like the case of without SO_2 . The NO conversion in the presence of SO_2 condition is lower at reaction temperature below 350°C and higher at reaction temperature beyond 350°C . An explanation of this phenomena can be explained using the acidity of the catalyst. The amount of Lewis acid site in the case of with SO_2 is less than in the case of without SO_2 at both lower and higher reaction temperature. This indicates that SO_2 affects the decreasing of Lewis acid site in the case of *co-25V5W* catalyst. [Sintarako (1998)]

The NO conversion after addition 10 vol.% H_2O , does not differ from the case of using feed gas without water in all temperature region. It is possible that tungsten oxide on catalyst surface can reduce the competitive adsorption of water and

ammonia. When added both SO_2 and H_2O to the reacting gas mixture, the behavior of this reaction is similar to the case of without SO_2 and H_2O .



สถาบันวิทยบริการ
จุฬาลงกรณ์มหาวิทยาลัย

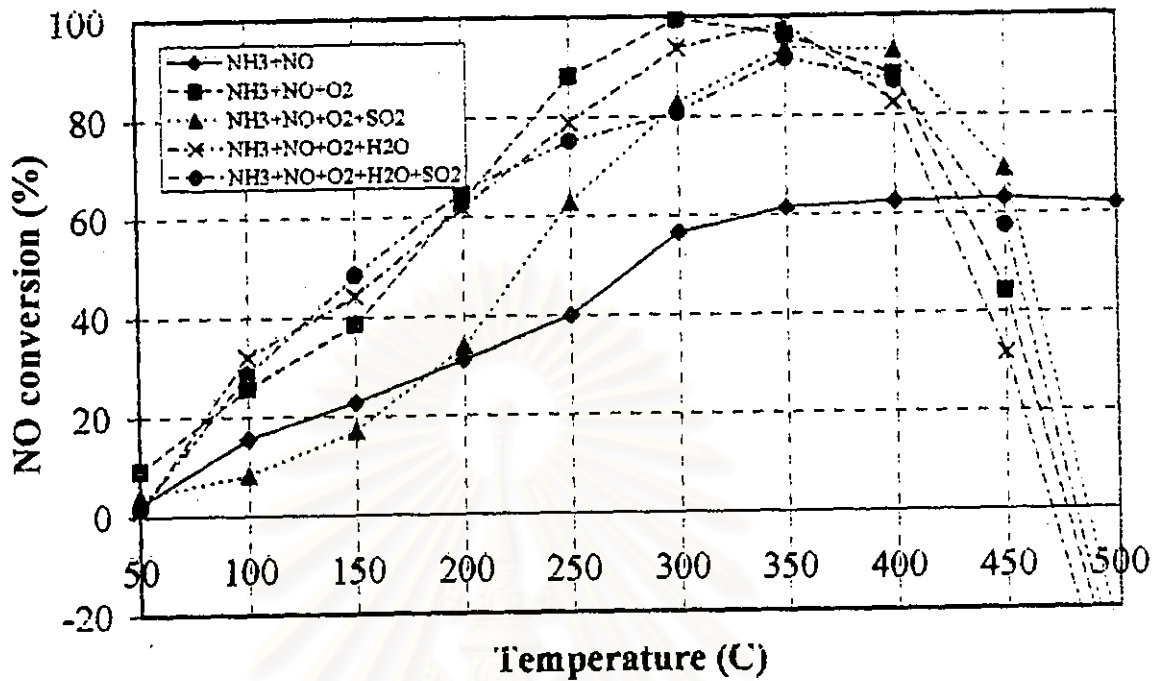


Figure 5.55: SCR activity of co-25V5W catalyst under several operating atmospheres

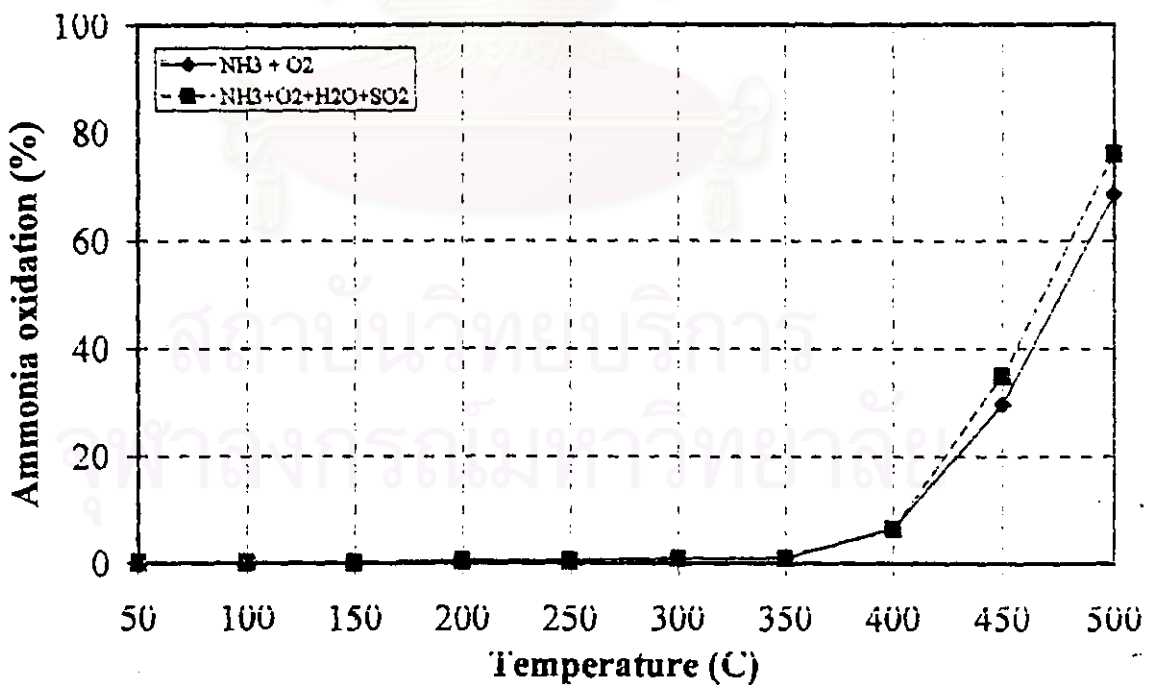


Figure 5.56: Ammonia oxidation reactions of co-25V5W catalyst

5.7.3 co-25V3K catalyst

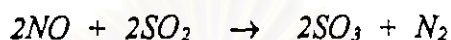
From the results described in sections 5.4 and 5.5, one can say that the NO conversion of co-25V3K catalyst differs from the base catalyst. Hence, this catalyst is used as an example for studying the behavior of a catalyst which potassium added. Figure 5.57 presents the NO conversion of co-25V3K catalyst under several operating conditions. The NO conversion of $\text{NO}+\text{NH}_3+\text{O}_2$ condition gradually increases with increasing reaction temperature until 500°C . Interestingly, NO conversion does not drop at higher temperature. Perhaps this behavior is related to ammonia oxidation reaction. Because the side reaction (NH_3+O_2) shows low value in conversion (about 10 %). The ammonia oxidation reaction of co-25V3K catalyst is depicted in figure 5.58.

For the catalyst in which SO_2 was added, the behavior is the same as 25V catalyst. Also, the reasons for this explanation like 25V catalyst too. [Sintarako (1998)] Surprisingly in the presence of water, the activity of the catalyst is higher than in the case of without water and becomes drop at higher temperature. It is possible that the competitive adsorption of water formed $-\text{OH}$ groups on catalyst surface which can generate the Brønsted acid site from surface vanadyl. [Ramis *et al.* (1990), Busca *et al.* (1998), Kamata *et al.* (1998)] The schemes of the generation of Brønsted acid sites are shown in section 3.3 previously (figure 3.2). Increasing of Brønsted acid site may play an important role for both SCR of NO with ammonia and ammonia oxidation. [Kijlstra *et al.* (1996), Kamata *et al.* (1998)]

Regarding the presence of both SO_2 and water, the NO conversion is similar to that of in the presence only water. But at higher temperature, the NO conversion of this catalyst significantly drops to bottom out at about 5 %. This behavior is not related to the ammonia oxidation in the presence of SO_2 and water. In the presence and absence of SO_2 and water conditions have highly differ in NO conversion (about 50 %) whereas in condition of ammonia oxidation reactions (NH_3+O_2 , $\text{NH}_3+\text{O}_2+\text{SO}_2+\text{H}_2\text{O}$) have small difference in NO conversion (about 20 %). Possibly,

the ammonia oxidation reaction is not a major factor of the drop in NO conversion in the presence of SO₂ and water condition.

Generation of SO₃ is an hypothesis that is proposed. SO₃ can be generated by the reaction of NO with SO₂.



From the difference in NO conversion, consequently, this hypothesis is tested. Figure 5.59 exhibits the NO conversion in NO + SO₂ condition. Similarly, the NO conversion can associate with the generation of SO₃. The result of testing this assumption, shows that NO can be reduced to nitrogen by oxidizing SO₂ to SO₃. The NO conversion gradually increases with increasing temperature until the maximum NO conversion is reached at temperature about 350°C and before decreasing at higher temperature.

In the same way, the result of NO + SO₂ condition can be used to explain the difference in NO conversion of the conditions with the presence and absence of water and SO₃ at higher temperature. One reason is the too high amount of SO₃ generation. SO₃ may cover catalyst surface and consequently leads to deactivation. In fact, this assumption should occur only in the presence of SO₂ and water condition. Because the V₂O₅/TiO₂ catalyst prefers to promote the SO₂ oxidation reaction to SO₃ than other reactions (exclude SCR reaction). [Waqif *et al.* (1992), Dunn *et al.* (1998)] Water added into the system may change the mechanism. As a result, NO may prefer to react with SO₂ than ammonia.

Another possible reason that can explain the drop of NO conversion in the presence of SO₂ and water condition is SO₃ accelerates the ammonia oxidation reaction at higher temperature. The supporting data is 25V5K catalyst that shows the negative value of NO conversion at higher temperature. However, both assumptions are too complicate for investigation. So that it should be investigated in detail in further research

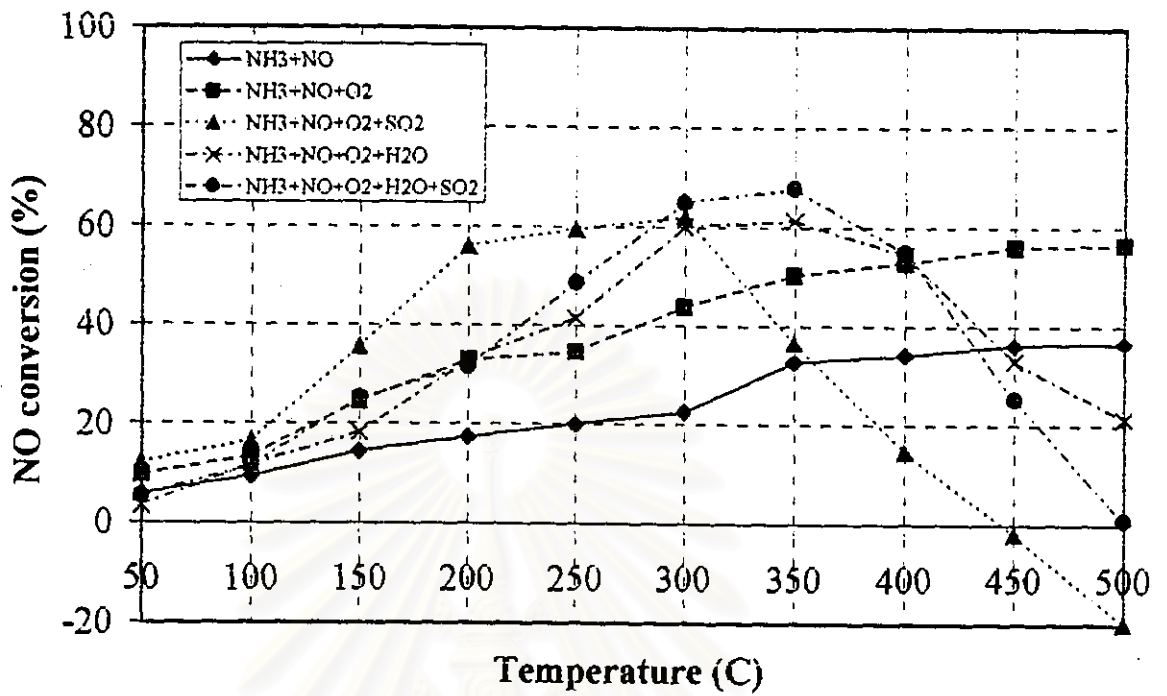


Figure 5.57: SCR activity of co-25V3K catalyst under several operating atmospheres

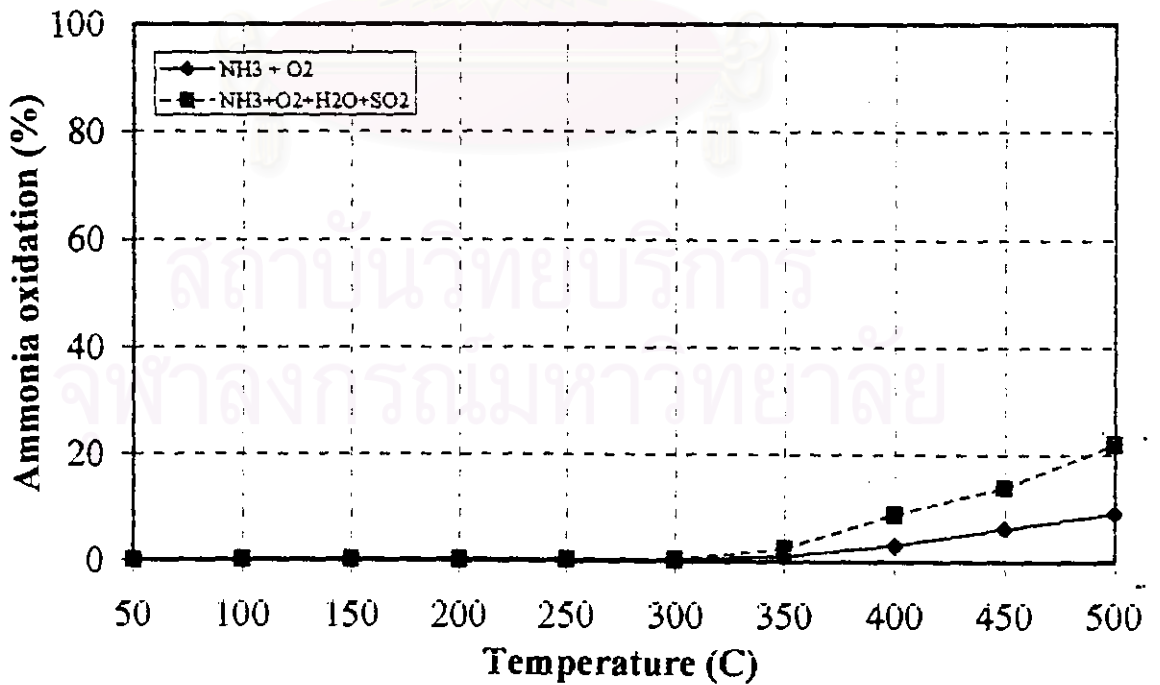


Figure 5.58: Ammonia oxidation reactions of co-25V3K catalyst

5.7.4 25V5W3K catalyst

The last catalyst tested is 25V5W3K catalyst. The behavior of this catalyst is similar to the based catalyst in all conditions ($\text{NO}+\text{NH}_3$, $\text{NO}+\text{NH}_3+\text{O}_2$, $\text{NO}+\text{NH}_3+\text{O}_2+\text{SO}_2$, $\text{NO}+\text{NH}_3+\text{O}_2+\text{H}_2\text{O}$, $\text{NO}+\text{NH}_3+\text{O}_2+\text{SO}_2+\text{H}_2\text{O}$, NH_3+O_2 and $\text{NH}_3+\text{O}_2+\text{SO}_2+\text{H}_2\text{O}$). Figure 5.60 and 5.61 represent the SCR activity and ammonia oxidation reactions of 25V5W3K catalyst, respectively.

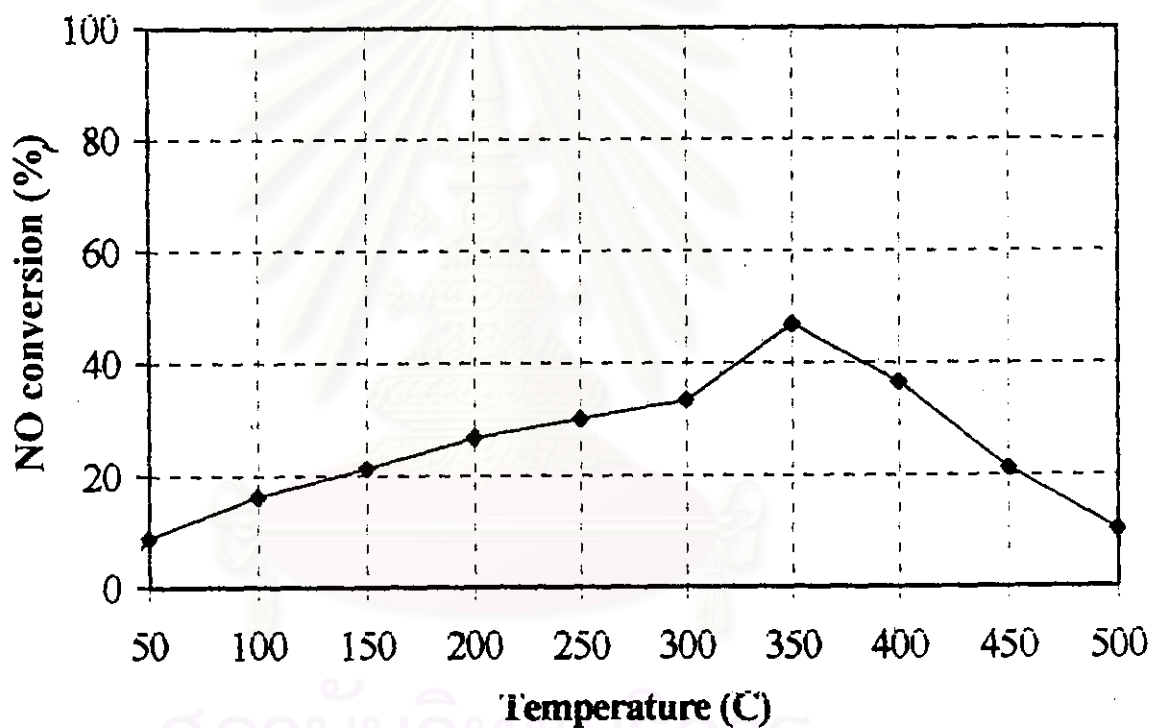


Figure 5.59: The NO conversion in NO + SO₂ condition

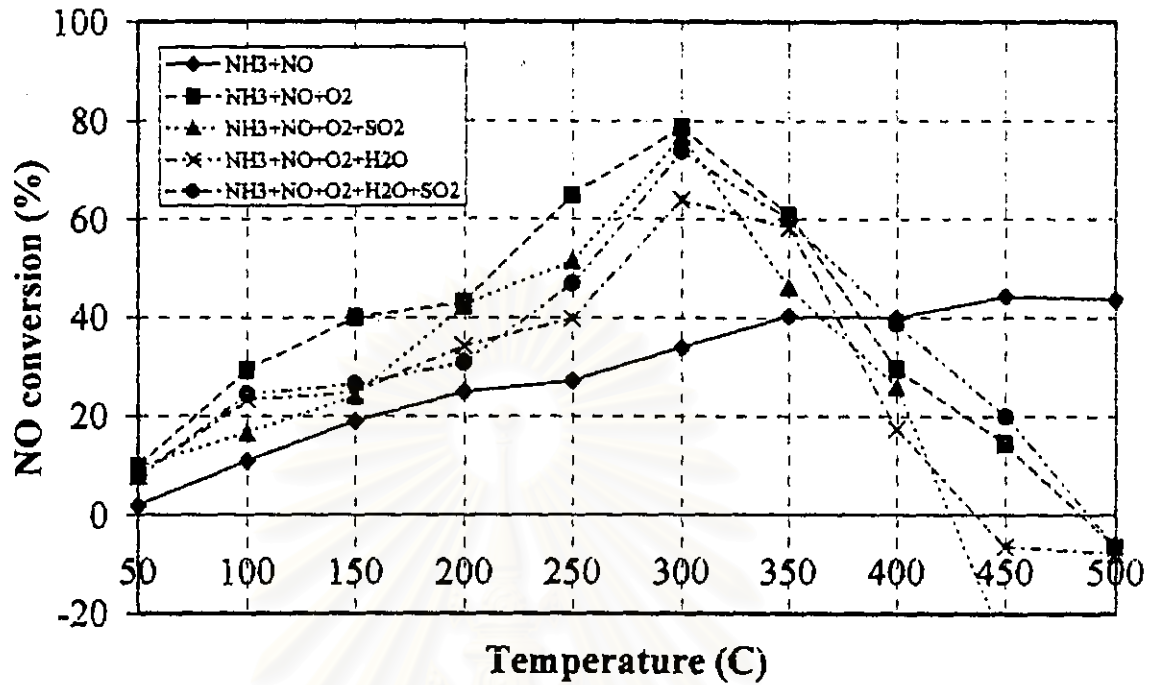


Figure 5.60: SCR activity of 25V5W3K catalyst under several operating atmospheres

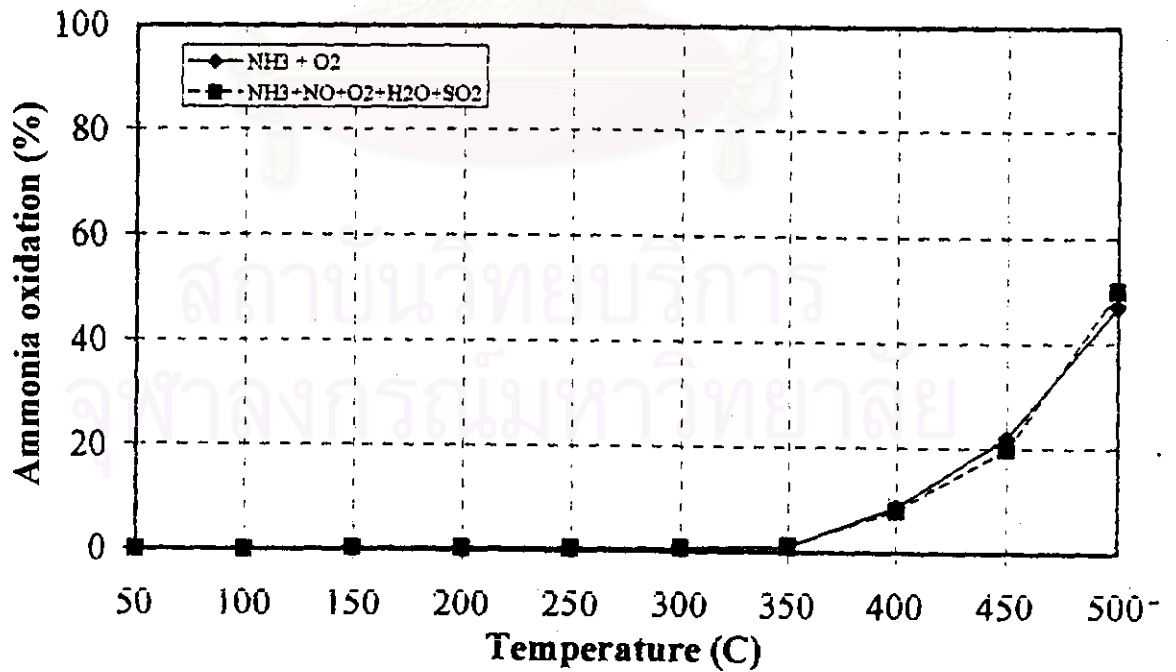


Figure 5.61: Ammonia oxidation reactions of 25V5W3K catalyst